

**An Investigation into Flow Mode Transition and
Development of Model for Pressure Drop Calculation in
Dense Phase Pneumatic Conveying System**

A Dissertation submitted

in partial fulfillment of the requirements for the
degree of

Master of Engineering

in

Thermal Engineering

by

Prabir Kumar Kar

Registration No.: 801483017

Under Supervision of

Dr. S.S. Mallick (Associate Professor)

&

Mrs. A. Mittal (Lecturer)



MECHANICAL ENGINEERING DEPARTMENT

THAPAR UNIVERSITY, PATIALA

July, 2016

CERTIFICATE

I hereby declare that the thesis entitled "An investigation into flow mode transition and development of model for pressure drop calculation in dense phase pneumatic conveying system" is an authentic record of my work carried out as requirements for the award of the degree of **Master of Engineering in Thermal Engineering at Thapar University, Patiala** under the supervision of **Dr. S.S. Mallick (Associate Professor)** and **Mrs. A. Mittal (Lecturer)**, Mechanical Engineering Department, Thapar University, Patiala during 21st July, 2014 to 5th July, 2016. No part of the matter embodied in this report has been submitted to any other university or institute for the award of any degree.

Date: 05/07/2016


Prabir Kumar Kar

It is certified that the above statement made by the student is correct to the best of my/our knowledge and belief.



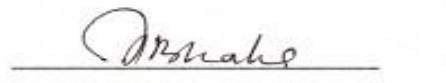
Dr. S.S. Mallick
Mechanical Engineering Department
Thapar University, Patiala - 147004



Mrs. A. Mittal
Mechanical Engineering Department
Thapar University, Patiala - 147004

Countersigned by


Head, Mechanical Engineering Department
Thapar University, Patiala - 147004


Dean of Academic Affairs
Thapar University, Patiala - 147004

Dedicated to
My Parents

Acknowledgements

I would like to express my deepest gratitude and indebtedness to my supervisor, Dr. S.S. Mallick and Mrs. A. Mittal for their excellent guidance, caring, patience, and providing me an excellent atmosphere for doing my research work. The opportunity, support, exposure and atmosphere provided by the Thapar University, Patiala, to carry out my studies are highly appreciated. A special debt of gratitude is owed to the authors whose works I have consulted and quoted in this work. Last but not least, I am forever grateful to my parents, family and friends for their unconditional support and best wishes.

I am really grateful to almighty for those joyful moments I enjoyed and painful instances which made me tough and strong to face situations in life to come and for the exceptional journey and memories at Thapar University, Patiala.

Prabir Kumar Kar

Abstract

This work presents an experimental investigation into the pneumatic conveying characteristics (PCC) for horizontal straight pipe section to address dense to dilute phase transition phenomenon and development of model for solids friction factor to predict the pressure drop throughout the pipeline for conveying of fine powders in fluidized dense phase. Pressure minimum curve (PMC) is the unique curve on the straight pipe pneumatic conveying characteristics (PCC) curve which indicates dense to dilute phase transition. An attempt has been made to address pressure minimum curve (PMC) by imposing constant Stokes number and constant solid loading ratio lines on straight pipe pneumatic conveying characteristics (PCC) curve. For reliable system design, accurate prediction of pressure drop throughout the pipeline is very important. Pressure drop occurs due to interaction between various phases of flow (e.g. gas-solid particles, particles-particles, particles-wall and gas-wall), mainly due to friction and momentum loss. In this article solids friction factor is modeled by using particle terminal velocity, Stokes number, solid loading ratio, average flow velocity, particle density and density of conveying medium by regression analysis. Fly ash (median particle diameter: 30 μm and 20 μm ; particle density: 2300 kg/m^3 and 2370 kg/m^3 ; loose-poured bulk density: 700 kg/m^3 and 660 kg/m^3) was conveyed through 65 mm I.D. \times 254 m (Fujian Longking Co.), 69 mm I.D. \times 168 m and 69 mm I.D. \times 554 m (University of Wollongong) pipelines and cement (median particle diameter: 19 μm ; particle density: 2910 kg/m^3 ; loose-poured bulk density: 1080 kg/m^3) was conveyed through 65 mm I.D.

× 254 m (Fujian Longking Co.), pipeline for wide range of air and solids flow rate. During fluidized dense phase conveying, a high concentration layer of material occupies the bottom portion of the pipeline. Where as in the upper portion of the pipeline, particles are suspended in conveying medium. Two-layer model is very much suitable to address fluidized dense phase flow phenomenon. In this study, solid friction factor is modeled by using terminal velocity and solid loading ratio for immature dune flow (initial stage of dune flow). For complete dune flow (e.g. two layer flow), solids friction factor is modeled by using existing "Weber A4" model with weightage factor τ_1 and newly developed model based on solid loading ratio, Stokes number and particle density to conveying medium density with weightage factor τ_2 . Where, the summation of τ_1 and τ_2 is 1.

Keywords: Pneumatic conveying, Dense phase, Pressure minimum curve, Pressure drop, Solids friction factor.

Contents

	Page No
List of Figures	viii
List of Tables	xiii
Nomenclature	xiv
1 Introduction and objectives	1
1.1 Introduction	1
1.2 Objectives	2
2 Literature review	3
2.1 Introduction	3
2.2 Pneumatic conveying and its components	3
2.3 Types of pneumatic conveying	4
2.4 Design consideration of pneumatic conveying	5
2.5 Minimum conveying velocity criteria	9
3 Evaluation of flow mode transition criteria	12
3.1 Introduction	12
3.2 Experimental data used in this study	14
3.3 Constant m^* lines plotted on straight pipe PCC	15
3.4 Constant Stokes number lines plotted on straight pipe PCC	21

3.5 Constant Stokes number lines plotted on total pipeline PCC	29
4 Modeling and validation of solid friction factor	34
4.1 Development of new model	34
4.2 Immature dune flow	35
4.3 Total pipeline predicted PCC according to "Immature dune flow model"	37
4.4 Two-layer flow	43
4.5 Total pipeline predicted PCC according to "Modified two-layer theory"	46
5 Conclusion and further scope of work	52
5.1 Conclusion	52
5.2 Future scope of work	53
REFERENCES	54
APPENDIX: A1	58

List of Figures

Figure 3.1	Layout of 65 mm I.D. × 254 m test rig at Fujian Longking Co. Ltd.	15
Figure 3.2	PCC for straight pipe (47.5 m) pressure (P ₆ -P ₉), cement, 65 mm I.D. × 254 m long pipeline	16
Figure 3.3	PCC for straight pipe (47.5 m) pressure (P ₆ -P ₉), fly ash, 65 mm I.D. × 254 m long pipeline	17
Figure 3.4	PCC for straight pipe (26.5 m) pressure (P ₆ -P ₉), fly ash, 80mm I.D. × 407 m long pipeline	18
Figure 3.5	PCC for straight pipe (26.5 m) pressure (P ₆ -P ₉), cement, 80 mm I.D. × 407 m long pipeline	18
Figure 3.6	PCC for straight pipe (52.68 m) pressure (P ₉ -P ₁₀), fly ash, 69 mm I.D. × 168 m long pipeline	19
Figure 3.7	PCC for straight pipe (26.91 m) pressure (P ₉ -P ₁₀), fly ash, 69 mm I.D. × 554 m long pipeline	20

Figure 3.8	PCC for straight pipe (47.5 m) pressure (P ₆ -P ₉), cement, 65 mm I.D. × 254 m long pipeline	22
Figure 3.9	PCC for straight pipe (47.5 m) pressure (P ₆ -P ₉), fly ash, 65 mm I.D. × 254 m long pipeline	22
Figure 3.10	PCC for straight pipe (26.5 m) pressure (P ₆ -P ₉), cement, 80 mm I.D. × 407 m long pipeline	23
Figure 3.11 :	PCC for straight pipe (26.5 m) pressure (P ₆ -P ₉), fly ash, 80 mm I.D. × 407 m long pipeline	23
Figure 3.12	PCC for straight pipe (52.68 m) pressure (P ₉ -P ₁₀), fly ash, 69 mm I.D. × 168 m long pipeline	24
Figure 3.13	PCC for straight pipe (40.41 m) pressure (P ₁₁ -P ₁₂), fly ash, 69 mm I.D. × 168 m long pipeline	25
Figure 3.14	PCC for straight pipe (26.91 m) pressure (P ₉ -P ₁₀), fly ash, 69 mm I.D. × 554 m long pipeline	26
Figure 3.15	PCC for straight pipe (26.91 m) pressure (P ₁₁ -P ₁₂), fly ash, 69 mm I.D. × 554 m long pipeline	26
Figure 3.16	PCC for straight pipe (40.10 m) pressure (P ₉ -P ₁₀), fly ash,	27

	105 mm I.D. × 168 m long pipeline	
Figure 3.17	PCC for straight pipe (44.50 m) pressure (P_{11} - P_{12}), fly ash,	28
	105 mm I.D. × 168 m long pipeline	
Figure 3.18	PCC for cement, 65 mm I.D. × 254 m long pipeline	29
Figure 3.19	PCC for cement, 80 mm I.D. × 407 m long pipeline	30
Figure 3.20	PCC for fly ash, 65 mm I.D. × 254 m long pipeline	30
Figure 3.21	PCC for fly ash, 80 mm I.D. × 407 m long pipeline	31
Figure 3.22	PCC for fly ash, 69 mm I.D. × 168 m long pipeline	32
Figure 3.23	PCC for fly ash, 69 mm I.D. × 554 m long pipeline	32
Figure 3.24	PCC for fly ash, 105 mm I.D. × 168 m long pipeline	33
Figure 4.1	Immature dune flow of fine powders in partially dense phase conveying	36
Figure 4.2	Experimental versus predicted PCC for cement 65 mm I.D. × 254 m long pipeline	38
Figure 4.3	Experimental versus predicted PCC for fly ash 65 mm I.D. × 254 m long pipeline	38
Figure 4.4	Experimental versus predicted PCC for cement	39

	80 mm I.D. × 407 m long pipeline	
Figure 4.5	Experimental versus predicted PCC for fly ash	40
	80 mm I.D. × 407 m long pipeline	
Figure 4.6	Experimental versus predicted PCC for fly ash	41
	69 mm I.D. × 168 m long pipeline	
Figure 4.7	Experimental versus predicted PCC for fly ash	42
	69 mm I.D. × 554 m long pipeline	
Figure 4.8	Two-layer flow of fine powders in dense phase	43
Figure 4.9	Experimental versus predicted PCC for cement	46
	65 mm I.D. × 254 m long pipeline	
Figure 4.10	Experimental versus predicted PCC for fly ash	47
	65 mm I.D. × 254 m long pipeline	
Figure 4.11	Experimental versus predicted PCC for cement	48
	80 mm I.D. × 407 m long pipeline	
Figure 4.12	Experimental versus predicted PCC for fly ash	49
	80 mm I.D. × 407 m long pipeline	
Figure 4.13	Experimental versus predicted PCC for fly ash	50

69 mm I.D. × 168 m long pipeline

Figure 4.14 Experimental versus predicted PCC for fly ash

51

69 mm I.D. × 554 m long pipeline

List of Tables

Table 3.1	Physical properties of conveyed product	14
-----------	---	----

Nomenclature

A	= Cross section area of the pipe [m ²]
B	= Bend loss factor
C	= Particle velocity in suspension [m/s]
D	= Internal diameter of pipe [m]
d _s	= Particle diameter [m]
d ₅₀	= Median particle diameter [μm]
$Fr = V/(gD)^{0.5}$	= Froude number of flow
Fr _i	= Froude number at pipe inlet
$Fr_m = V_m/(gD)^{0.5}$	= Mean Froude number related to the section of pipe
$Fr_p = V/(gd_s)^{0.5}$	= Particle Froude number based on superficial air velocity and particle diameter
$Fr_s = w_{fo}/(d_s g)^{0.5}$	= Froude number of particle related to particle diameter
f _r	= Sliding friction factor between solids and pipe wall
g	= Acceleration due to gravity [m ² /s]
L	= Length of pipe [m]
L _h	= Horizontal length of pipe [m]
L _v	= Vertical length of pipe [m]
m _f	= Mass flow rate of conveying air [kg/s]

m_s	= Mass flow rate of solids [kg/s]
$m^* = m_s/m_f$	= Solids loading ratio
$m_{s(\text{non-sus})}$	= Mass flow rate of solids being conveyed in non-suspension layer in dense phase regime [kg/s]
$m_{s(\text{sus})}$	= Mass flow rate of solids being conveyed in suspension layer in dense phase regime [kg/s]
N	= Number of bends
ΔP	= Pressure drop through straight horizontal pipe section [Pa]
ΔP_{acc}	= Pressure drop due to initial acceleration [Pa]
ΔP_b	= Pressure drop through a bend [Pa]
ΔP_T	= Total pipe line pressure drop [Pa]
ΔP_v	= Pressure drop due to vertical section [Pa]
$Re = \rho VD/\mu$	= Reynolds number of gas
$Re_p = \rho_s Vd_s/\mu$	= Reynolds number for particle
St	= Stokes number
V	= Superficial air/gas velocity [m/s]
$V_{i,\text{min}}$	= Minimum conveying air velocity requirement at pipe inlet [m/s]
ε	= Void fraction of the strand
ρ	= Density of air [kg/m ³]
ρ_m	= Mean air density [kg/m ³]
ρ_s	= Particle density [kg/m ³]

ρ_{bl}	= Loose-poured bulk density [kg/m ³]
λ_{bs}	= Solids friction factor through bends
λ_f	= Air only friction factor
λ_s	= Solids friction factor through straight pipe
$\beta = w_f/V$	= Velocity ratio related to particle fall velocity in a cloud
w_f	= Particle settling velocity in a cloud [m/s]
τ_1	= Shear stress on the pipe wall due to non-suspension layer in dense phase regime [Pa]
τ_2	= Shear stress on the pipe wall due to suspension layer in dense phase regime [Pa]
μ	= Dynamic viscosity of air [Pas]

Subscripts

e	= Equivalent
f	= Fluid (air)
h	= Horizontal
i	= Inlet condition
min	= Minimum

Acronyms

I.D.	≡	Internal diameter of pipe
PCC	≡	Pneumatic conveying characteristics

Chapter 1

Introduction and Objectives

1.1 Introduction

Pneumatic conveying system deals with transportation of wide variety of dry powdered and granular solids in a gas stream. The system requirements are a source of compressed gas, usually air, a feed device, a conveying pipeline and a receiver to discharge the conveyed material and carrier gas. Pneumatic conveying systems can be categorized into two types : dilute phase and dense phase conveying. In dilute phase conveying gas velocity is sufficiently high so that the particles are in suspension, but in dense phase conveying the material is conveyed at low velocity in a non-suspension mode. In dense phase conveying two types of flow can be categorized. One is moving bed flow, in which material is conveyed in dunes along with the bottom of the pipeline, another is slug or plug type flow, in which material is conveyed through full bore plugs separated by air gaps. Although dilute phase pneumatic conveying system has countless advantages over alternative mechanical conveying systems for transportation of materials, they do have some drawbacks like particle degradation and erosive wear of pipeline bends. Many researchers work on development of pneumatic conveying systems for conveying wide range of material in dense phase with low conveying velocity. Various empirical power function based models have been developed for calculating solid friction factor by various researchers (Wypych, 1994; Jones and Williams, 2003; Mallick, 2009 and Setia, 2014). Pneumatic conveying characteristics (PCC) is a representation of mass flow rate of conveying air versus pressure drop for a given product that is being conveyed pneumatically through a particular pipeline. Although

numerous PCCs for the total pipeline have been published over the years by various researchers, limited work has been carried out to study the straight-pipe PCC for modeling dense to dilute phase transition criteria for fine powders. Therefore further studies are to be carried out to address dense to dilute transition criteria (e.g. using "Straight-pipe" PCC) with the help of constant Stokes number and constant m^* lines for fluidized dense phase conveying. Accurate prediction of pressure drop throughout the pipeline is of paramount importance from the point view of a well-designed system. Therefore the aim is to present a reliable modeling and scale-up method for the precise prediction of pressure drop for dense as well as dilute phase pneumatic conveying of fine powders. According to two-layer model suspended solid particles are moved over the non-suspended partially static layer. In case of moving bed flow a dune type pattern on the bed surface could be observed. However, according to definition of Stokes number it is very much sufficient to model particle-particle/wall interaction for a non-suspension layer. In this study, Combination of "Weber A4" model and newly developed model using Stokes number for modeling solid friction factor provides better prediction of pressure drop.

1.2 Objectives

The following specific objectives are

- (i) Experimental investigation on change in flow mechanism (dense phase to dilute phase) along the flow direction in straight pipe with the help of constant Stokes number and constant m^* lines.
- (ii) To develop an empirical model for calculate pressure drop in dense phase pneumatic conveying of fine powders.
- (iii) Modification of two layer model to improve its accuracy.

Chapter 2

Literature Review

2.1 Introduction

In this chapter some basic components of pneumatic conveying system have been reviewed. Various researchers have investigated on the design considerations of pneumatic conveying system to make it more optimized.

2.2 Pneumatic conveying and its components

Pneumatic conveying systems are generally very simple and extremely acceptable for transportation of wide variety of powdered and granular materials in several factories, sites and plants. The system needs a source of compressed gas, basically air, a feeding device, a conveying pipeline and a receiver bin. The beauty of pneumatic conveying system is totally enclosed and that's why it provides dust-free transportation, flexibility in routing (can take vertical lift and any inclined bend) and also multiple pick-up and discharge point. High, low or negative pressure can be used for conveying bulk solid materials. Generally dry air is used for conveying hygroscopic materials, but for explosive materials inert gas (nitrogen) is used. However, dilute phase pneumatic conveying has some disadvantages. It requires high power consumption and wear, abrasion of the equipments also particle degradation etc. are the common problem. One thumb

rule for pneumatic conveying is that the inner diameter of the conveying pipeline must be at least three times larger than the largest size of material to be conveyed to prevent blockage inside the pipeline (Klinzing, 1990). Pneumatic conveying system comprises of four well defined zones. The four distinct zones are described as follows

- **The Prime Mover :** The prime mover is a very crucial component of pneumatic conveying system. An extensive range of compressors, blowers, fans and vacuum pumps are used to supply the required energy to the conveying medium.
- **Feeding, Mixing and Acceleration Zone :** In this distinct zone the bulk solids are injected into the conveying medium. Initially the bulk solid particles are at rest condition but a huge change in momentum occurs when the solids are combined with conveying medium. This momentum change provides the acceleration of the static bulk solid particles.
- **The Conveying Zone :** The conveying zone comprises of piping arrangement, it can have several number of bends, inclined section as well as vertical lift. Pipe materials must be selected in such a way that friction losses and particle degradation remain as low as possible.
- **Gas-Solids Separation Zone :** This zone is responsible for separating bulk solids from the conveying medium. There are several systems like bag house filter, cyclone separator etc are generally used for separation purpose.

2.3 Types of Pneumatic Conveying

There are several ways to classify a pneumatic conveying system, but most appropriate classification is based on average particle concentration along the pipeline. According to that there are two discrete categories as follows

- **Dilute Phase :** In dilute phase conveying the bulk solid particles are in suspension mode along the pipeline. Due to that a relative high conveying medium velocity is required throughout the pipeline. One of the most important advantages of dilute phase system is that it can convey any material. There are also some disadvantages like it consumes too much power, pipe wear is high also there is high particle degradation etc.

- **Dense Phase** : Dense phase conveying comprises of Dune flow and Slug or Plug type flow. Dune flow is basically moving bed flow, in which the bulk solid particles are conveyed in the form of dunes along the bottom of the pipeline. However, in Plug flow the bulk solid materials are conveyed as full bore plugs separated by air gaps. For Plug flow there is one thumb rule that is the conveyed material should have enough permeability.

2.4 Design consideration of pneumatic conveying

For designing pneumatic conveying system one should keep in mind two important parameters. One is "minimum pressure drop along the pipeline", another is "minimum conveying velocity throughout the pipeline". Due to minimum conveying velocity there is less chance of pipe wear as well as particle degradation. There are various research works on these two important parameters; some of them are discussed below :

Pressure drop prediction throughout the pipeline is very much important to determine compressor size (for positive pressure conveying). Barth (1958) proposed a relation (Eq. 2.1) for calculating the pressure drop along the straight pipe.

$$\Delta p = (\lambda_f + m^* \lambda_s) L \rho V^2 / 2D \quad (2.1)$$

The above equation has also been used by several researchers like Stegmaier (1987), Rizk (1976,1982), Wypych (1989), Pan (1992), Pan and Wypych (1998), Jones and Williams (2003), Mallick (2009) and Setia (2014).

Chamber and Marcus (1986) calculated the total pipeline pressure drop by adding the segmental pressure drop (Eq. 2.2 to 2.6). The segments are as follow straight pipes, bend loss, vertical lift loss and loss due to initial acceleration. According to them

$$\text{Acceleration loss : } \Delta P_{acc} = \rho V^2 (1 + 2m^* C/V) / 2 \quad (2.2)$$

$$\text{Vertical loss : } \Delta P_v = m^* \rho g L_v V / C \quad (2.3)$$

$$\text{Straight pipe loss : } \Delta P = (\lambda_f + m^* \lambda_s) L \rho V^2 / 2D \quad (2.4)$$

$$\text{Bend loss : } \Delta P_b = NB(1 + m^*) \rho V^2 / 2 \quad (2.5)$$

$$\text{Total loss : } \Delta P_T = \Delta P_{acc} + \Delta P_v + \Delta P + \Delta P_b \quad (2.6)$$

They used Stegmaier (1978) model for calculating solid friction factor (Eq. 2.7)

$$\lambda_s = 2.1m^{*-0.3} Fr^{-1} Fr_s^{0.25} (D/d) 0.1 \text{ for } d < 0.5 \text{ mm} \quad (2.7)$$

Klinzing et al. (1989) evolved a correlation for calculating solid friction factor in horizontal pneumatic conveying, based on unified theory of Yang. Three types of glass particles (two spherical and one crushed; d as 67, 450 and 900 μm ; ρ_p as 2470, 2395 and 2464 kg/m^3) one iron ore flake (d as 400 μm ; ρ_p as 5004 kg/m^3) were conveyed through two horizontal pipes with I.D. 0.0266 m and 0.0504 m. Using Yang's unified theory they found the co-relation for calculating solids friction factor (Eq. 2.8).

$$\lambda_s = 3C_{ds}\varepsilon^{-4.7} \rho(V-C)^2 D / 4(\rho_p - \rho) d C^2 \quad (2.8)$$

As per the Newton's regime drag coefficient (C_{ds}) is 0.44 and pressure drop is obtained (Eq. 2.9) as

$$\Delta P_s / L = 2 \lambda_s \rho_p C^2 (1 - \varepsilon) / D \quad (2.9)$$

When they compared the results obtained from the above models with results from experimental data they found that the overall standard relative deviation (SRD) is obtained as 42.1%.

Stegmaier (1978) developed a power function based model for calculating solids friction factor. Where various fine and coarse particles like fly ash, alumina, quartz powder, sand etc with particle size ranging from 15 to 112 μm and particle density ranging from 1500 to 4100 kg/m^3 were used as the test materials and the model as Eq. (2.10).

$$\lambda_s = 2.1(m^*)^{-0.3} (Fr)^{-2} (Fr_s)^{0.5} (D/d_s)^{0.1} \quad (2.10)$$

Weber (1981) delivered another model which is the modified form of Stegmaire model for calculating solids friction factor (Eq. 2.11) by modification of particle Froude number as

$$\lambda_s = 2.1(m^*)^{-0.3}(Fr)^{-2}(Fr_{sD})^{0.5}(D/d_s)^{0.1} \quad (2.11)$$

Wypych et al. (1990) performed further experimentation into long distance conveying of fine pulverised coal ($d_{50} = 21 \mu\text{m}$; $\rho_s = 1495 \text{ kg/m}^3$). They proposed a power function based model for calculating solids friction factor (Eq. 2.12) as

$$\lambda_s = (m^*)^{-0.4555}(F_{rm})^{-1.13419}(\rho_m)^{-0.2931}(D)^{-0.1088} \quad (2.12)$$

Rizk (2006) provides a new model (Eq. 2.13) for pressure drop and solids friction factor calculation as

$$\Delta P_s/L = 0.5\mu \lambda_s Fr^2 \rho_{fg} \quad (2.13)$$

where λ_s (Eq. 2.14) as

$$\lambda_s = \lambda_{ifr}^*(C/V) + 2\beta/Fr^2(C/V) \quad (2.14)$$

From the above equation three boundaries can be derived as (Eq. 2.15 to 2.17)

Case 1: Gas velocity very high (solid loading ratio is very less)

$$\lambda_s = \lambda_{ifr}^*(C/V) \quad (2.15)$$

Case 2: Gas velocity lower (Gas velocity above saltation velocity)

$$\lambda_s = \lambda_{ifr}^*(C/V) + 2\beta/Fr^2(C/V) \quad (2.16)$$

Case 3: Gas velocity below saltation (dunes and plugs)

$$\lambda_s = \lambda_{fr}^*(C/V) \quad (2.17)$$

Cai et al. (2011) investigate on the effect of moisture content on the conveying characteristics. They used lignite and soft coal as the test material and maximum conveying pressure was 4 MPa. They found that when the moisture content of the test material increases the mass flow rate decreases accordingly. For lignite and soft coal mass flow rate varies respectively $3.24 \% < M < 8.18 \%$ and $0.4 \% < M < 6.18 \%$. They observed that flow ability of lignite was better than flow ability of soft coal. They proposed that as the moisture content increases electrostatic force decreases due to conductivity of water and liquid bridge of the coal particles. That's why pressure drop of soft coal was larger than lignite for similar operating conditions.

Rinoshika and Suzuki (2010) installed soft fins in the horizontal pipeline of pneumatic conveying system and found that this arrangement can reduce the pressure drop and conveying air velocity and also the power consumption. They used polyethylene of particle diameter 2.3 mm as the test material. Due to the oscillating characteristics of soft fins the maximum reduction rates of minimum pressure drop velocity, critical velocity and power consumption by using soft fin are about 15 %, 13 % and 23 % respectively compared to conventional pneumatic conveying system. The high speed camera and image processing were used to measure the oscillating characteristics of different soft fins. Basically the soft fins provide the perpendicular component of velocity as a result the particles remains in suspension mode throughout the pipeline.

Mallick et al. (2009) investigated on the two layer model on the basis of actual flow condition in dense phase. They proposed that there is an interface between the suspension and non-suspension layers. The two layer model (Eq. 2.18) as

$$\Delta P = (L/A)(\tau_1 S_1 + \tau_2 S_2) \quad (2.18)$$

$$\tau_1 = 0.5(\lambda_{\text{non-sus}})(\rho_{\text{non-sus}})V^2 \quad (2.19)$$

For the suspension layer (Barth,1958)

$$\tau_2 = 0.5(\lambda_f + m*\lambda_{\text{sus}})\rho V_1^2 \quad (2.20)$$

Whereas λ_{sus} can be found out from "modified Weber A4 model" (Eq. 2.21)

$$K1 = [\{(V-C)/w_{fo}\}^2 2(C/V)/(\lambda_s Fr^{*2})]^{0.5} \quad (2.21)$$

Setia et al. (2014) investigated on solids friction factor and developed a new model based on VLR (volume loading ratio). For dense phase conveying it is considered that some bottom portion of the pipeline is occupied by the conveying product so, the pipe volume available for the flow of air and solid particles is substantially decreased. To address this partial occupancy of pipe volume by solids, a volumetric loading ratio term is suggested as (Eq. 2.22)

$$VLR = \{(m_s/\rho_s)/(m_f/\rho_f)\} \quad (2.22)$$

From a wide range of straight pipe pressure drop data for fly ash for pipe line 69 mm I.D. × 168 m, ESP dust for 69 mm I.D. × 554 m, the following model was derived by using superficial gas velocity and volume loading ratio term as (Eq. 2.23)

$$\lambda_s = 0.114(V)^{-1.87}(VLR)^{-0.51} \quad (2.23)$$

2.5 Minimum conveying velocity criteria

Dense to dilute phase transition criteria is basically assigned by the location of PMC in the straight pipe PCC. Matsumoto (1974) studied on the minimum conveying velocity through different pipelines diameters respectively 29 mm and 49 mm, by using glass bead, copper bead and polystyrene as the test materials. According to their experimental results they provided the following co-relation (Eq. 2.24) for minimum velocity for dilute phase

$$V_{\min} = 3.4\sqrt{gD} (\rho/\rho_p)^{0.294}(Ut/\sqrt{gD})^{1.02} m^{*0.277} \quad (2.24)$$

Weber (1981) investigated on minimum conveying velocity as followed by the equation (Eq. 2.25 to 2.26)

For $U_t \leq 3$ m/s

$$Fr_i = [7 + 8/3U_t]m^{*0.25}(d/D)^{0.1} \quad (2.25)$$

For $U_t \geq 3 \text{ m/s}$

$$Fr_i = 15m^{*0.25}(d/D)^{0.1} \quad (2.26)$$

Schade (1987) investigated on minimum conveying velocity for different diameters of pipelines from 50 mm to 150 mm by using test materials as sand, styropor, rubber and polystyrol. According to experimental results he found a power function based co-relation (Eq. 2.27)

$$V_{\min} = 2.8G_s^{0.1}D^{0.428}d^{-0.023}\rho_p^{0.306}\rho^{-0.405} \quad (2.27)$$

Cabrejos and Klinzing (1994) investigated on minimum conveying velocity through 50 mm pipeline for conveying of alumina, glass beads and polyester polymers. According to their model PMC can be predicted as (Eq. 2.28)

$$V_{\min} / \sqrt{gD} = U_t / \sqrt{gD} + 0.00224(\rho_p/\rho)^{1.25}(m^*)^{0.5} \quad (2.28)$$

Kalman et al. (2005) investigated on PMC of straight pipe PCC with the help of particle Reynolds number (Re_p^*) and Archimedes number (Ar) for conveying of glass beads, zirconium, alumina, iron, ammonium oxide. They found that (Eq. 2.29 to 2.31)

For $Ar > 16.5$

$$Re_p^* = 5Ar^{3/7} \quad (2.29)$$

For $0.45 < Ar < 16.5$

$$Re_p^* = 16.7 \quad (2.30)$$

For $Ar < 4.5$

$$Re_p^* = 21.8Ar^{1/3} \quad (2.31)$$

Bansal et al. (2013) provided a new model by using Buckingham π theorem for predicting PMC with the help of particle Reynolds number and Archimedes number. Conveyed product as fly ash (particle density as 2300 kg/m^3 , bulk density as 700 kg/m^3 and d_{50} as $30 \text{ }\mu\text{m}$) and white powder (particle density as 1600 kg/m^3 , bulk density as 620 kg/m^3 , d_{50} as $55 \text{ }\mu\text{m}$) were

transported through 105 mm I.D. 168 m, \times 69 mm \times 148 m and 69 mm \times 554 m long pipeline.
The co-relation provided (Eq. 2.32 and 2.33)

For fly ash,

$$Re_p = 8.027Ar^{1.001} \quad (2.32)$$

For white powder,

$$Re_p = 1.694Ar^{1.004} \quad (2.33)$$

Where

$$Re_p = \rho d V_{PMC} / \mu$$

$$Ar = \rho^2 d^3 g (\rho_p - \rho) / \rho \mu^2$$

Many researchers (Weber, 1981; Schade , 1987; Cabrejos and Klinzing, 1994; Kalman et al., 2005 and Bansal et al., 2013;) investigated on prediction of pressure drop with the help of solids friction factor and several power function based models.

Chapter 3

Evaluation of Flow Mode Transition Criteria

3.1 Introduction

Many researchers (Wypych, 1989; Mill, 2004; Ratnayake and Datta, 2007; Mallick, 2009; Setia, 2014) investigated on total pipeline conveying characteristics for fine powders. But a very little amount of work is done for straight pipe conveying characteristics for fine powders in fluidized dense phase. Pressure minimum curve is the unique curve that indicates the dense to dilute phase transition criteria in a straight pipe PCC. There are several methods to allocate the PMC. With such background, the paramount motivation of this section is to analyze the straight pipe conveying characteristics for several powders, pipelines and pipeline tapping points and achieve a superior comprehension of flow mode transition criteria with the help of constant solid loading ratio lines and constant Stokes number lines. Stokes number is basically a non dimensional number, it is the ratio of particle (dispersed phase) relaxation time to the characteristics time scale of flow. To calculate particle entrainment characteristics, the interaction level between the dispersed phase and the continuous phase must be determined. This interaction can be explained by a series of “coupling” precisely: one-way coupling, two-way coupling, and four-way coupling. The one-way coupling happen during very low particle loading cases, in which the effect of dispersion is dominated by turbulent effects while the transfer of momentum from the particles to the flow is not significant due to the low concentration. The two-way coupling arises when the particle loading is sufficiently high that there is enough momentum transfer between the particles and the turbulent phase in addition to the standard interaction of the fluid to the particles. This region can be further divided into ranges in which the effect on turbulence is dampening or enhancing. For cases in which the Stokes number of the particle is small, the

added surface area allows a higher level of momentum transfer, thereby dissipating the turbulence (i.e. acts as a damper). Larger diameter particles can introduce additional vortex shedding and add to the turbulent energy produced (Elghobashi, 1994). The final scale encompasses both the fluid's effect on the particles and the particle's effect on the fluid, but also introduces the effect of particle collisions. This phase is typically only encountered for very dense flows where a granular effect becomes significant. Recently the quantification of turbulence statistics due to fine particles has been discussed with the help of Stokes number. Turbulence channel flow is characterized by the flow Reynolds number as well as the length and time scale of turbulence. This is because the turbulent flows are miscellaneous multi scale phenomena. If the particles are introduced in to the turbulence channel flows, the succeeding major quantities should be considered:

- Ratio of particle density to fluid density
- The particle Reynolds number
- The drag co-efficient of particles
- The ratio of the particle diameter to the length scale of turbulence
- The ratio of particle time scale to the time scale of turbulence i.e. the Stokes number.

3.2 Experimental data used in this study :

a) Fly ash (Wypych et al., 2005; Mallick, 2009)

b) Fly ash (Setia et al., 2014)

c) Cement (Setia et al., 2014)

Table 3.1: Physical properties of conveyed products

Product	ρ_s (kg/m³)	ρ_{bl} (kg/m³)	d_{50} (μm)
Fly ash (Mallick et al., 2009)	2300	700	30
Fly ash (Setia et al., 2014)	2370	660	22
Cement (Setia et al., 2014)	2910	1080	19

Fly ash was conveyed through 69 mm I.D. \times 168 m, 105 mm \times 168 m and 69 mm I.D. \times 554 m long pipeline by Mallick et al., (2009) at the Bulk Material Handling Laboratory of the University of Wollongong, Australia. Another kind of fly ash and cement were conveyed through 65 mm \times 254 m and 80 mm \times 407 m long pipeline by Setia et al., (2014) at the pneumatic conveying test facilities of Fujian Longking Co. (China). A schematic of the test set up for 65 mm I.D. \times 254 m long pipeline is shown in fig 3.1. The test rig comprises of

- 0.7 m³ bottom-discharge blow tank feeding system;
- 65 mm I.D \times 254 m long mild steel pipeline, including 2.7 m and 13.4 m vertical lift, nine 1 m radius 90° bends;
- A receiver bin of 2 m³ capacity;

- The receiver bin and blow tank were supported on shear beam type load cells to provide data of mass flow rates for solids. P1, P2 and P3 are the pressure transducers;
- A portable data acquisition system for data recording and analysis.

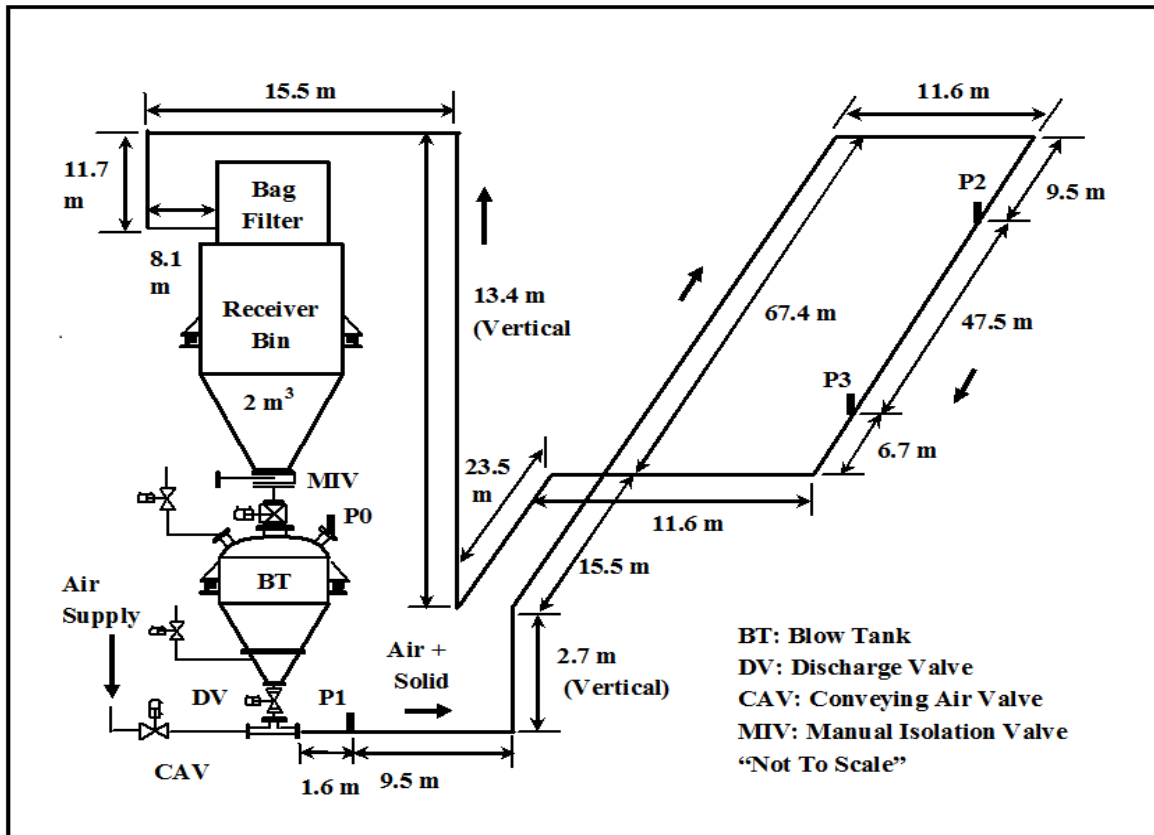


Figure 3.1: Layout of 65 mm I.D. × 254 m test rig at Fujian Longking Co. Ltd.

3.3 Constant m^* lines plotted on straight pipe PCC

Application of "straight pipe" static pressure measurement data from the respective pipelines and tapping locations over a large bandwidth of steady-state conveying condition, the PCC for the straight pipe sections were obtained for various bulk solids flow rate

- Straight pipe (47.5 m) pressure (P_6 - P_9), cement, 65 mm I.D. × 254 m long pipeline
- Straight pipe (47.5 m) pressure (P_6 - P_9), fly ash, 65 mm I.D. × 254 m long pipeline
- Straight pipe (26.5 m) pressure (P_6 - P_9), fly ash, 80 mm I.D. × 407 m long pipeline

- d) Straight pipe (26.5 m) pressure (P₆-P₉), cement, 80 mm I.D. × 407 m long pipeline
- e) Straight pipe (52.68 m) pressure (P₉-P₁₀), fly ash, 69 mm I.D. × 168 m long pipeline
- f) Straight pipe (26.91 m) pressure (P₉-P₁₀), fly ash, 69 mm I.D. × 554 m long pipeline

Solid loading ratio (m^*) is basically the ratio of mass flow rate of conveying air versus mass flow rate of conveying solid particles. Pneumatic conveying characteristics (PCC) is a representation of mass flow rate of conveying air versus pressure drop for a given product that is being conveyed pneumatically through a particular pipeline. The steps for allocating constant m^* lines are to calculate m^* for all the experimental data points first and then with the help of interpolation plotting of constant m^* lines take place.

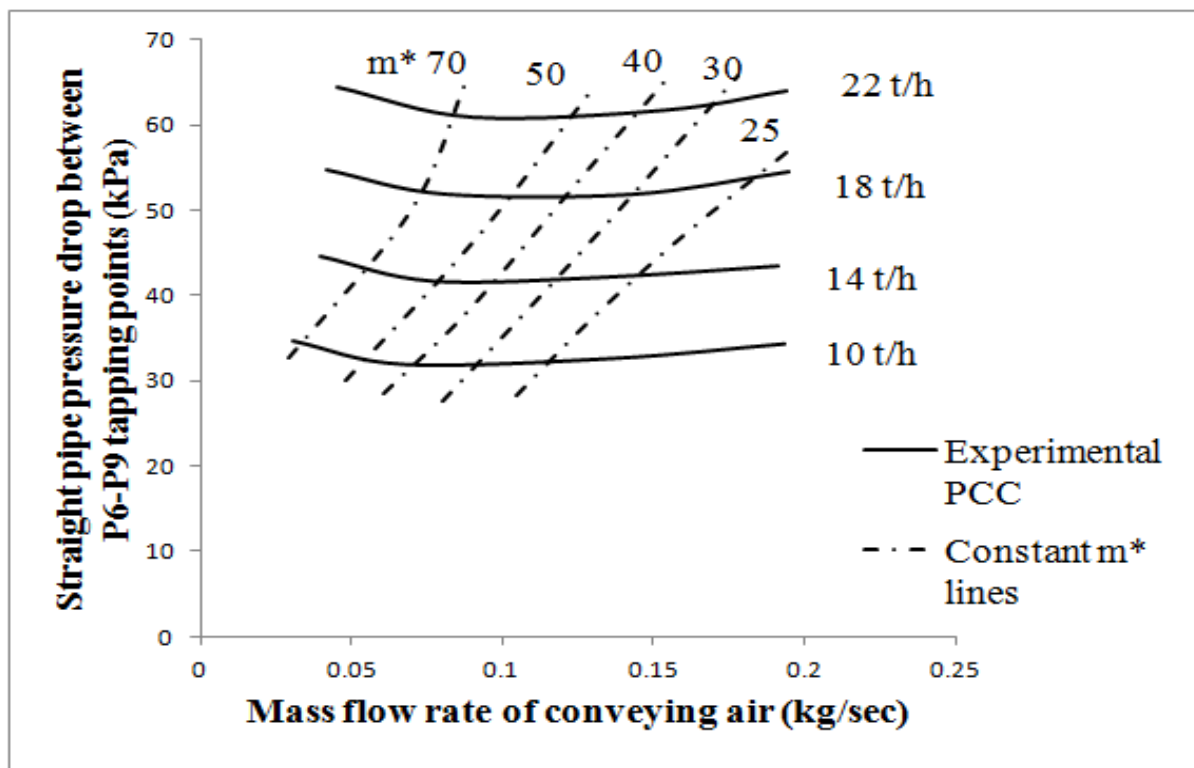


Figure 3.2: PCC for straight pipe (47.5 m) pressure (P₆-P₉), cement, 65 mm I.D. × 254 m long pipeline

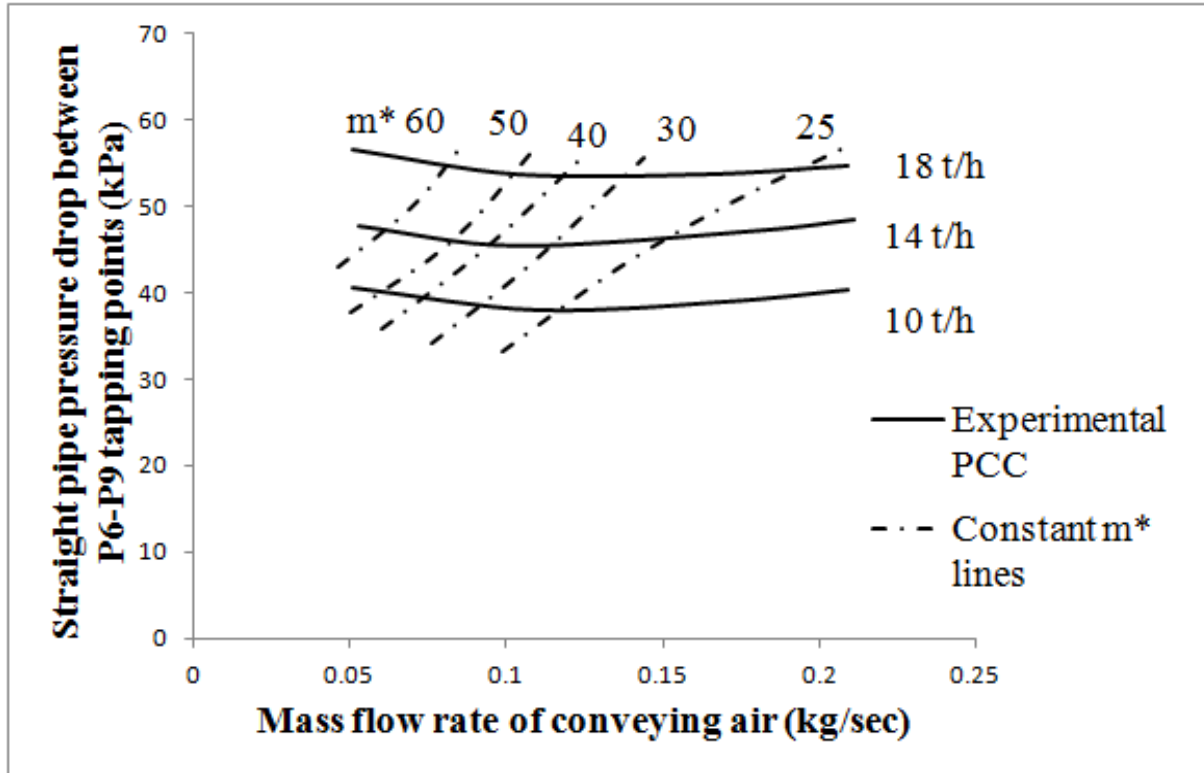


Figure 3.3: PCC for straight pipe (47.5 m) pressure (P_6 - P_9), fly ash, 65 mm I.D. \times 254 m long pipeline

The PCC is drawn employing the experimental data for cement conveying through 65 mm I.D. \times 254 m long pipeline. The straight pipe pressure drop is used between pressure tapping P_6 and P_9 and the distance between two pressure transducer is 47.5 m. Pressure drop per unit length is used in Y- axis and mass flow rate of conveying air per second is taken on the X- axis as shown in Figure 3.2. The PCC presents that the inclination of pressure drop per unit length at first decreases, then change in slope becomes low, after that change in slope increases. Basically, an ideal PCC has U shape curve where PMC can be defined very clearly. Here this PCC is not an ideal PCC but, it follows the ideal U trend. In this PCC probably the constant m^* line range between 60 to 50 indicates the PMC. Same trend was also observed for the PCC drawn using the experimental data for fly ash, 65 mm I.D. \times 254 m long pipeline, as shown in Figure 3.3. the constant m^* line range between 55 to 50 probably indicates the PMC.

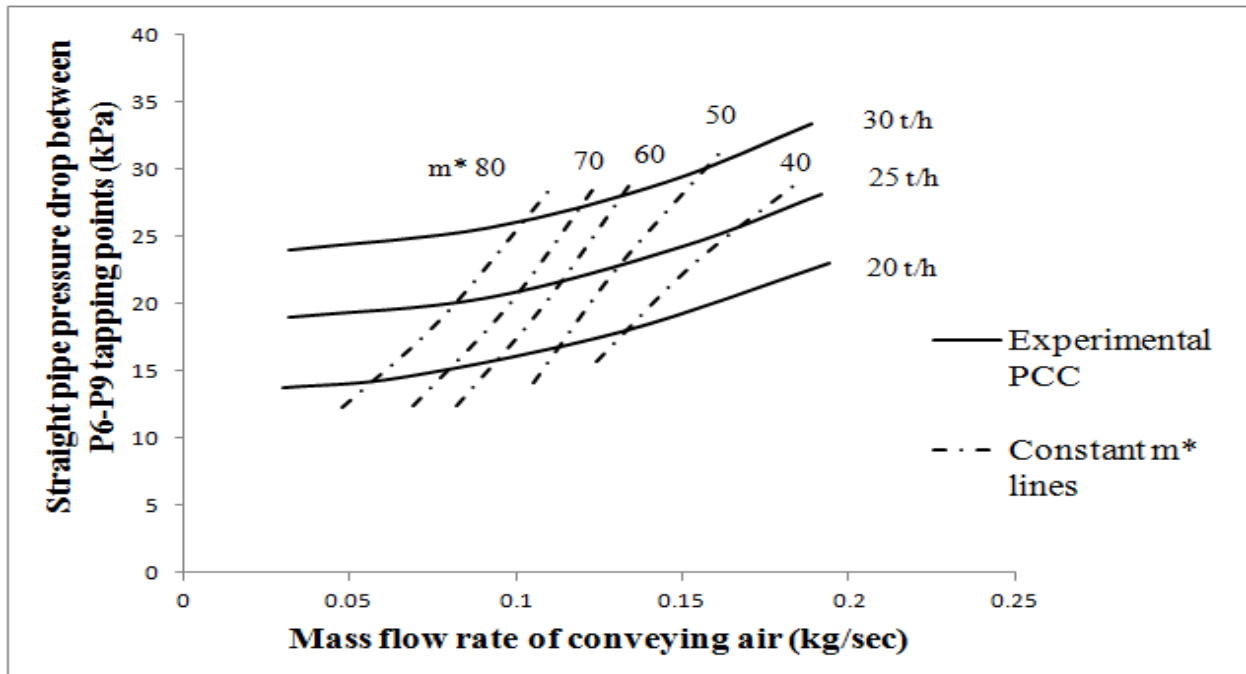


Figure 3.4: PCC for straight pipe (26.5 m) pressure (P_6 - P_9), fly ash, 80 mm I.D. \times 407 m long pipeline

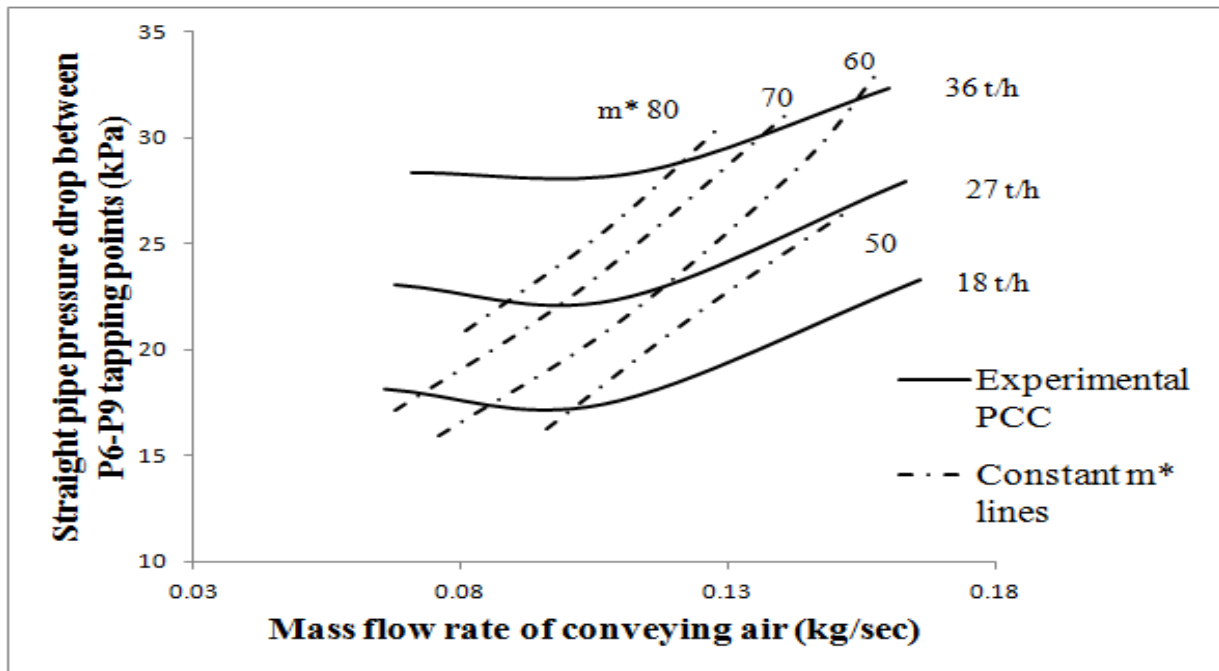


Figure 3.5: PCC for straight pipe (26.5 m) pressure (P_6 - P_9), cement, 80 mm I.D. \times 407 m long pipeline

The PCC provided in figure 3.4 and 3.5 contains constant m^* lines for fly ash, 80 mm I.D. \times 407 m long pipeline for P6 - P9 tapping points, horizontal length was 26.5 m. As the mass flow rate of conveying air increases the straight pipe pressure drop per unit length increases and it reaches maximum around 35 kPa. For, both the cases the constant m^* line range between 75 to 65 probably indicates the PMC.

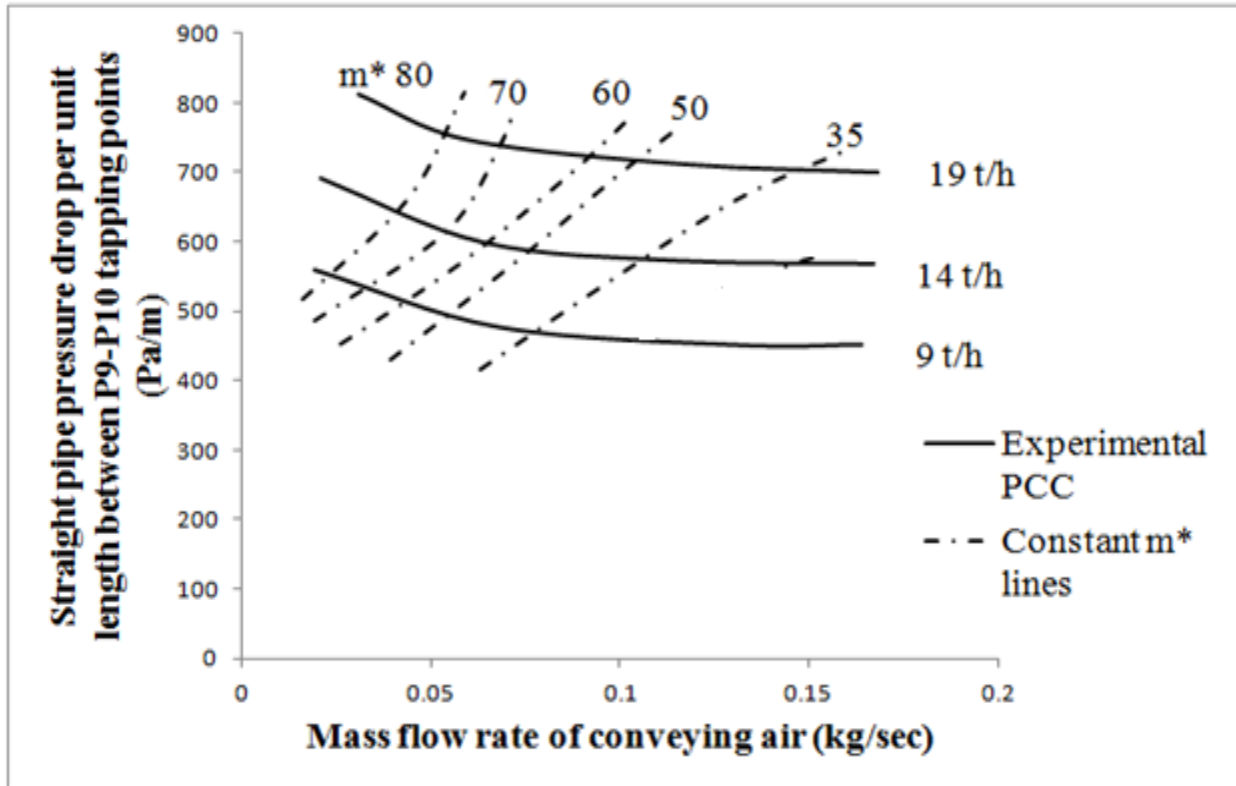


Figure 3.6: PCC for straight pipe (52.68 m) pressure (P_9 - P_{10}), fly ash, 69 mm I.D. \times 168 m long pipeline

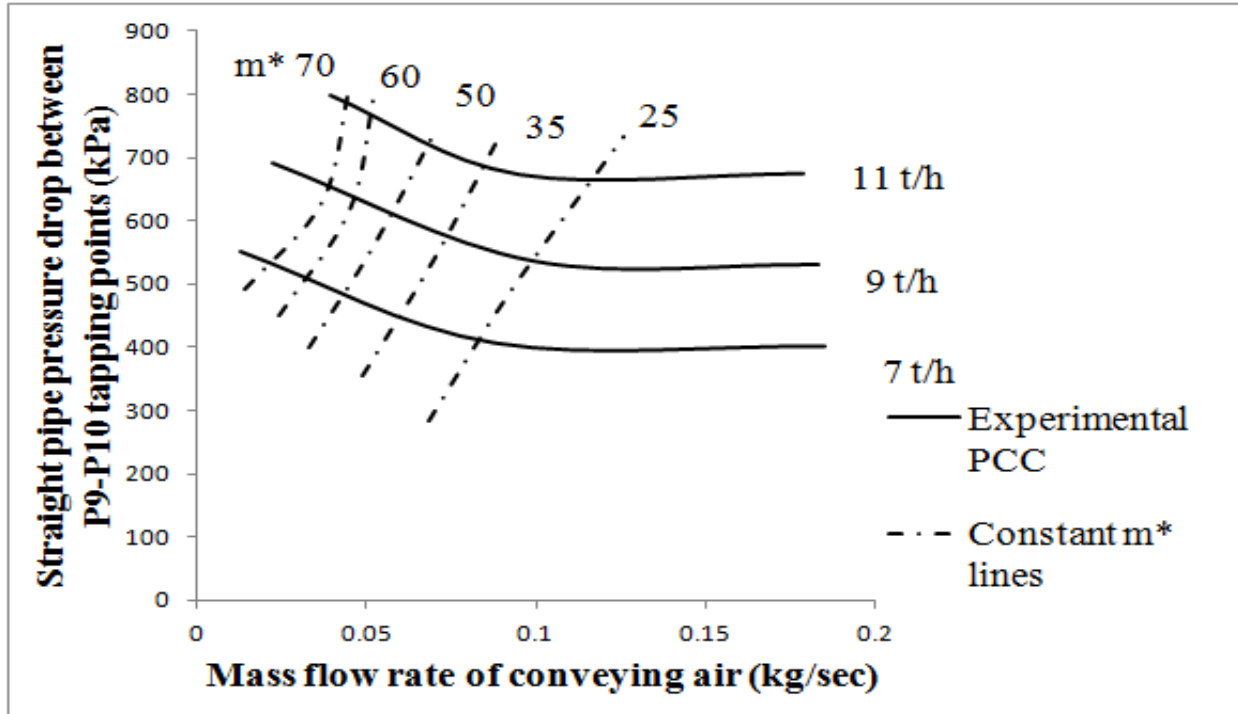


Figure 3.7: PCC for straight pipe (26.91 m) pressure (P₉-P₁₀), fly ash, 69 mm I.D. × 554 m long pipeline

The PCC presented in figure 3.6 and 3.7 presents the slope of the m_s lines decreases when the mass flow rate of conveying air was low, but as the mass flow rate of conveying air increases the gradual decreasing slope of m_s lines became stable. For, fly ash, 69 mm I.D. × 168 m long pipeline constant m^* line ranges from 75 to 65 probably indicates the PMC. For fly ash, 69 mm I.D. × 554 m long pipeline constant m^* line ranges from 35 to 25 probably indicates the PMC.

3.4 Constant Stokes number lines plotted on straight pipe PCC

Application of "straight pipe" static pressure measurement data from the respective pipelines and tapping locations over a large bandwidth of steady-state conveying condition, the straight pipe pneumatic conveying characteristics were obtained for various bulk solids flow rate

- a) Straight pipe (47.5 m) pressure (P_6-P_9), cement, 65 mm I.D. × 254 m long pipeline
- b) Straight pipe (47.5 m) pressure (P_6-P_9), fly ash, 65 mm I.D. × 254 m long pipeline
- c) Straight pipe (26.5 m) pressure (P_6-P_9), cement, 80 mm I.D. × 407 m long pipeline
- d) Straight pipe (26.5 m) pressure (P_6-P_9), fly ash, 80 mm I.D. × 407 m long pipeline
- e) Straight pipe (52.68 m) pressure (P_9-P_{10}), fly ash, 69 mm I.D. × 168 m long pipeline
- f) Straight pipe (40.41 m) pressure ($P_{11}-P_{12}$), fly ash, 69 mm I.D. × 168 m long pipeline
- g) Straight pipe (26.91 m) pressure (P_9-P_{10}), fly ash, 69 mm I.D. × 554 m long pipeline
- h) Straight pipe (26.91 m) pressure ($P_{11}-P_{12}$), fly ash, 69 mm I.D. × 554 m long pipeline
- i) Straight pipe (40.1 m) pressure (P_9-P_{10}), fly ash, 105 mm I.D. × 168 m long pipeline
- j) Straight pipe (44.5 m) pressure ($P_{11}-P_{12}$), fly ash, 105 mm I.D. × 168 m long pipeline

Stokes number is basically a non dimensional number, it is the ratio of particle (dispersed phase) relaxation time to the characteristics time scale of flow. Recently the quantification of turbulence statistics due to fine particles has been discussed with the help of Stokes number.

$$St \text{ no} = \rho_d d_d^2 V_s / 18 \mu_c D$$

For $St \text{ no} \ll 1$, particle follow the continuous phase flow closely.

For $St \text{ no} > 1$, particles unaffected by continuous phase flow

The steps for allocating constant Stokes number lines are at first to calculate Stokes number for all the experimental data points and then with the help of interpolation plotting of constant Stokes number lines take place.

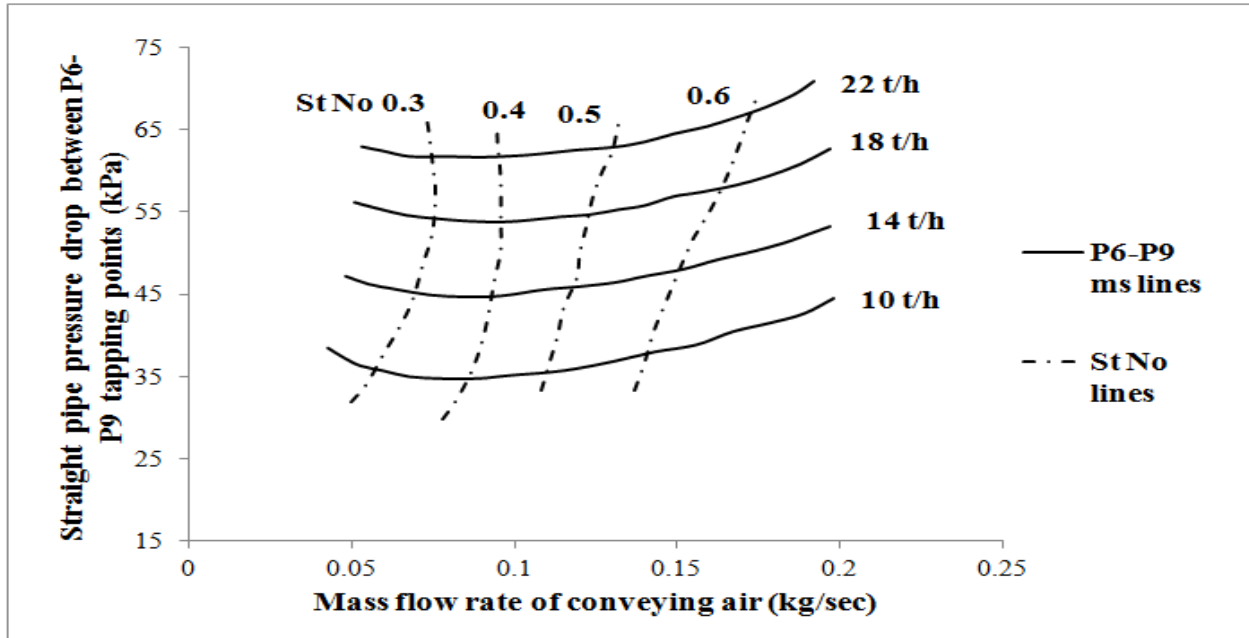


Figure 3.8: PCC for straight pipe (47.5 m) pressure (P_6 - P_9), cement, 65 mm I.D. \times 254 m long pipeline

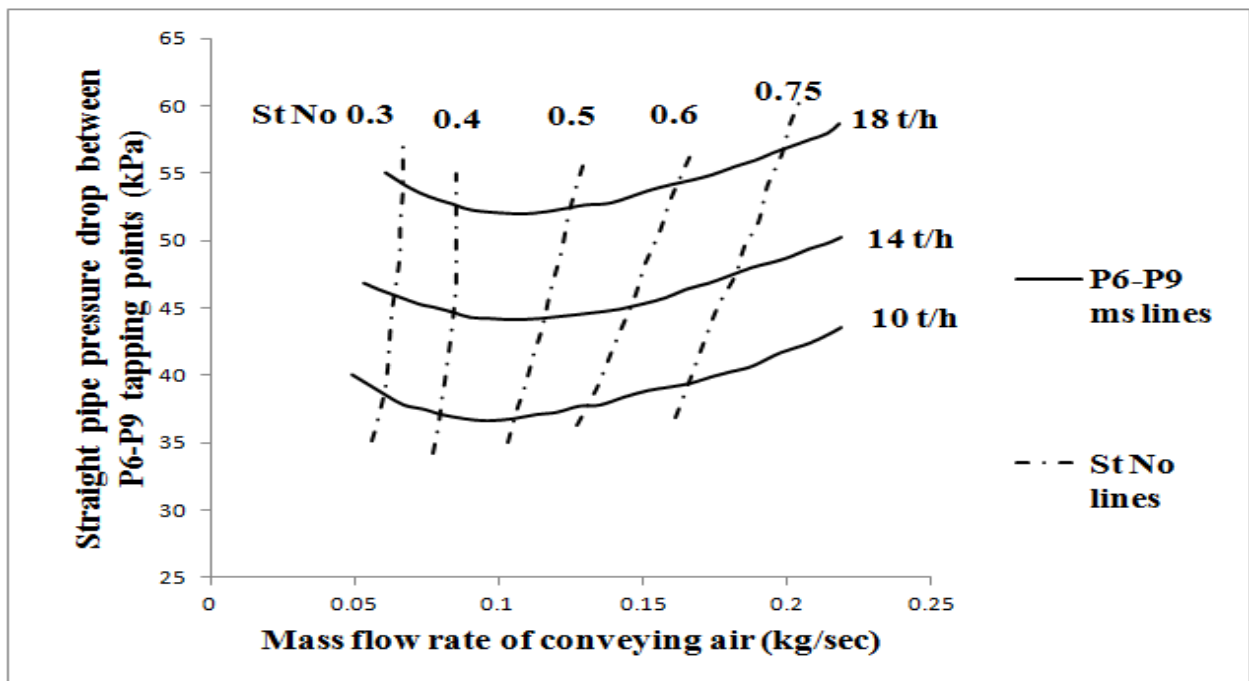


Figure 3.9: PCC for straight pipe (47.5 m) pressure (P_6 - P_9), fly ash, 65 mm I.D. \times 254 m long pipeline

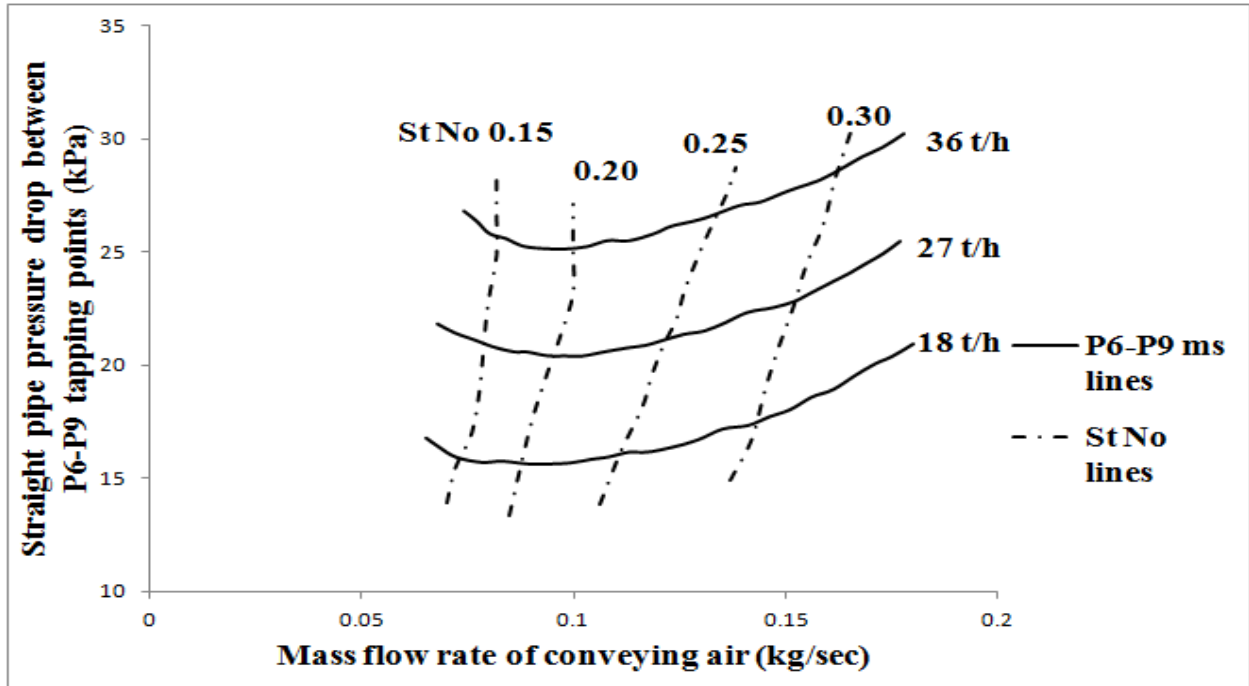


Figure 3.10: PCC for straight pipe (26.5 m) pressure (P_6 - P_9), cement, 80 mm I.D. \times 407 m long pipeline

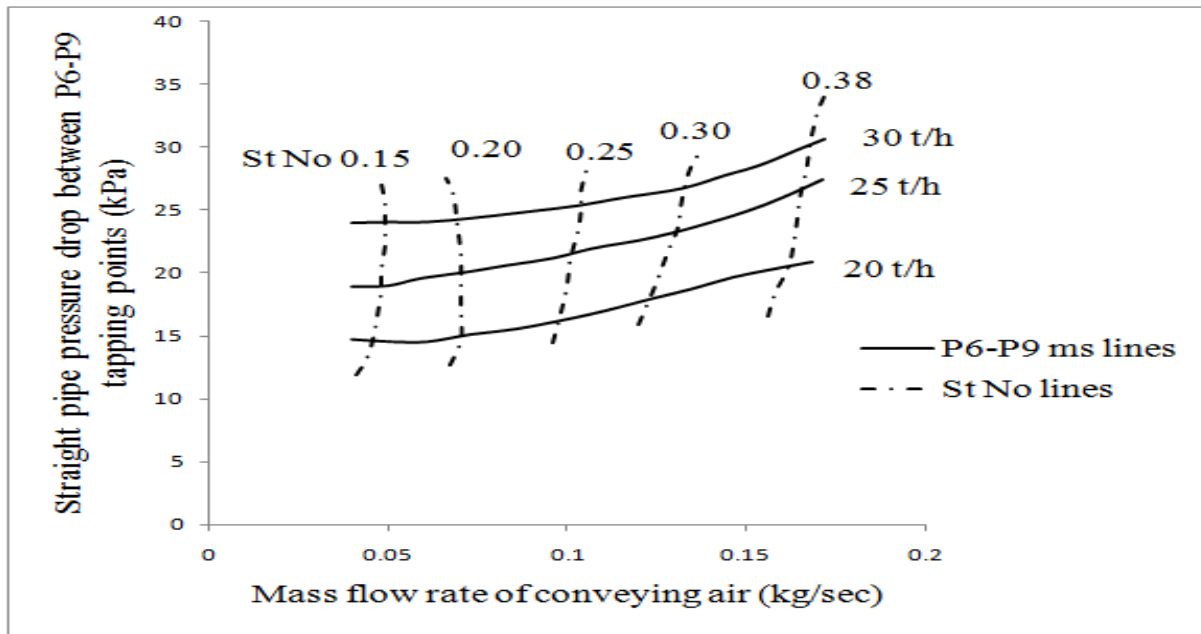


Figure 3.11: PCC for straight pipe (26.5 m) pressure (P_6 - P_9), fly ash, 80 mm I.D. \times 407 m long pipeline

Figures 3.8 and 3.10 show cases of conveying cement through pipelines of two different length and diameter. In the first case when diameter is 65 mm and length is 254 m, constant Stokes number line ranges between 0.4 to 0.5 indicating the PMC. However, for scale up condition when diameter is 80 mm and length is 407 m then constant Stokes number line ranging between 0.2 to 0.25 indicates the PMC.

From figure 3.9 and 3.11 it has been shown that for conveying fly ash through pipelines of two different length and diameter when the diameter is 65 mm and length is 254 m constant Stokes number line ranging from 0.4 to 0.5 indicates the PMC. Where as, for scale up condition when diameter is 80 mm and length is 407 m, constant Stokes number line ranging from 0.2 to 0.35 indicates the PMC.

According to four PCC discussed above it is found that irrespective of conveying material for 65 mm and length 254 m constant Stokes number line ranging from 0.4 to 0.5 indicates the PMC and when the diameter is 80 mm and length is 407 m, 0.2 to 0.35 indicates the PMC.

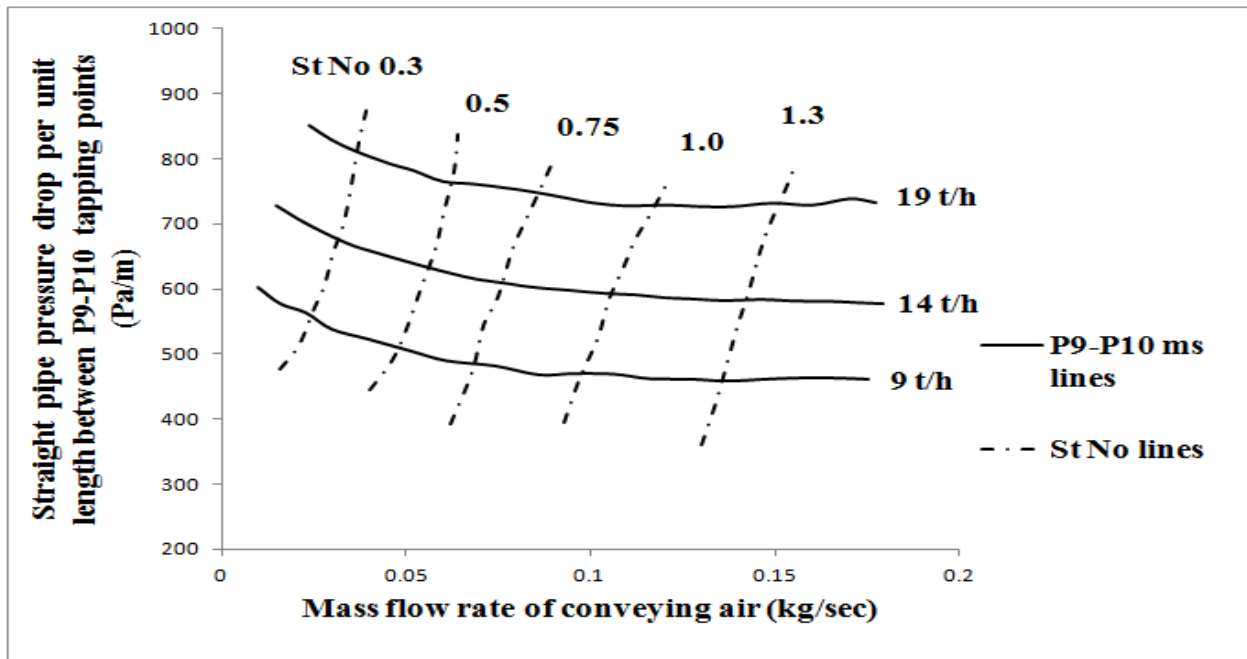


Figure 3.12: PCC for straight pipe (52.68 m) pressure (P_9 - P_{10}), fly ash, 69 mm I.D. \times 168 m long pipeline

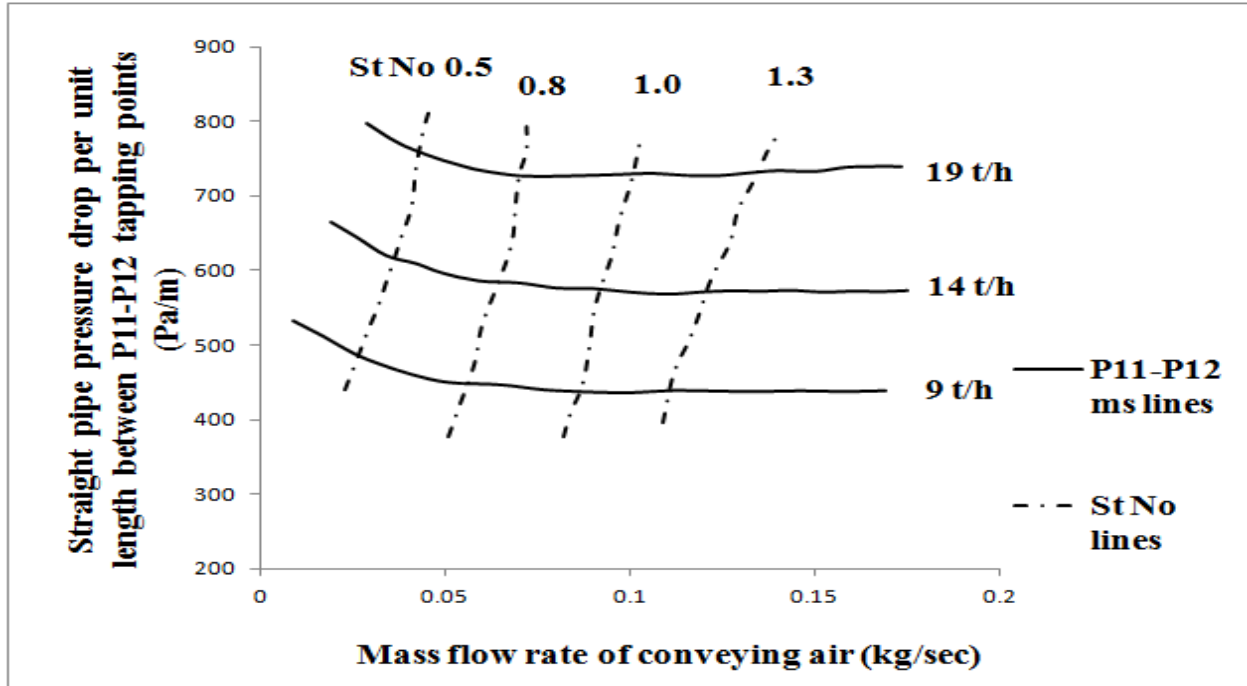


Figure 3.13: PCC for straight pipe (40.41 m) pressure (P_{11} - P_{12}), fly ash, 69 mm I.D. \times 168 m long pipeline

From the above two figures 3.12 and 3.13 it is found that same material is conveyed through same pipeline if the pressure tapping location changes the range of constant Stokes number line to allocate PMC also changes. For figure 3.12 constant Stokes number line ranges between 0.45 to 0.55 and figure 3.13 constant Stokes number line ranges between 0.50 to 0.65 and indicates the PMC.

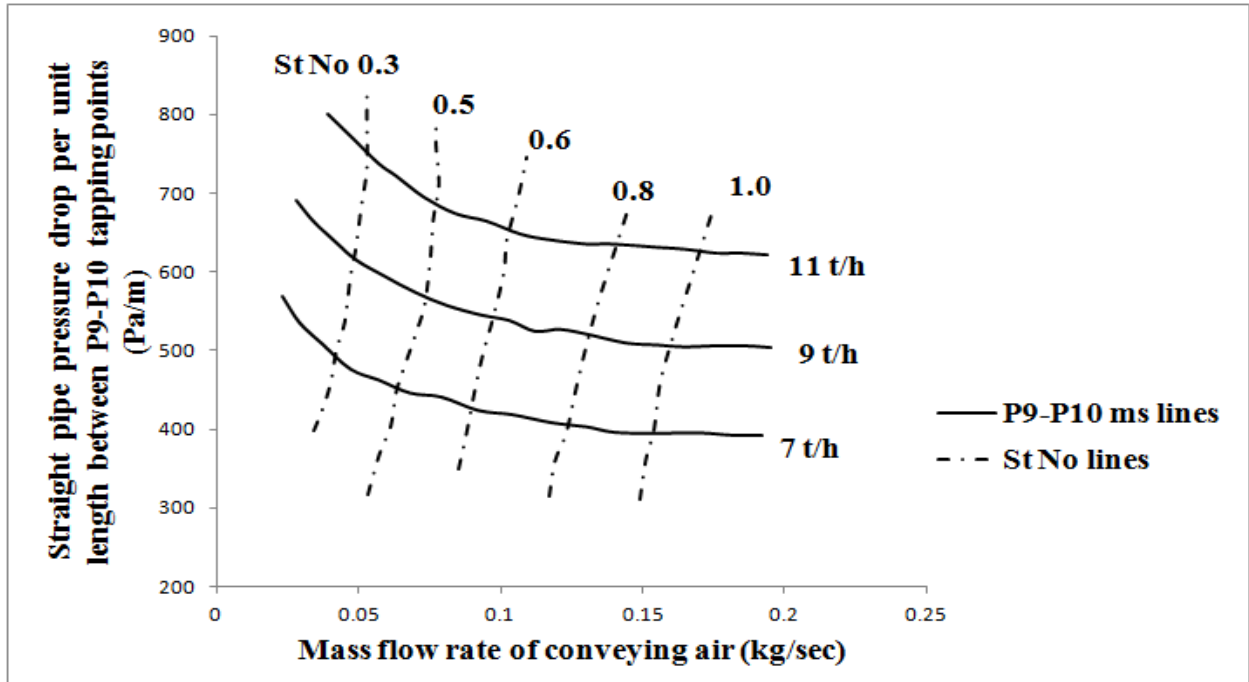


Figure 3.14: PCC for straight pipe (26.91 m) pressure (P₉-P₁₀), fly ash, 69 mm I.D. × 554 m long pipeline

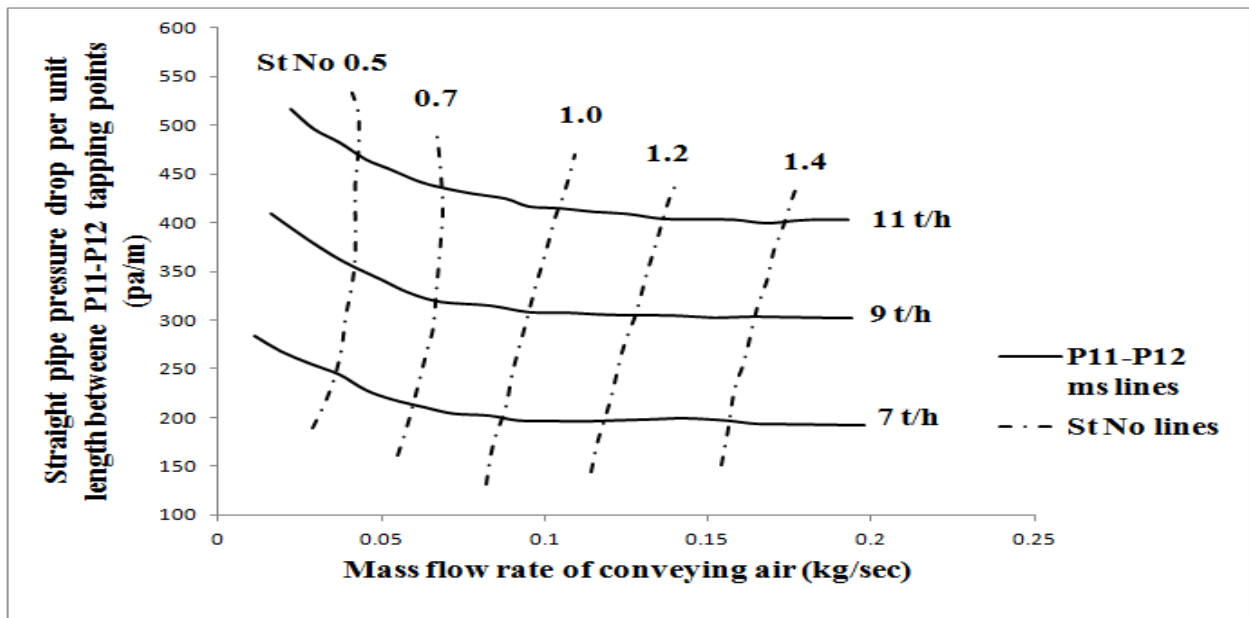


Figure 3.15: PCC for straight pipe (26.91 m) pressure (P₁₁-P₁₂), fly ash, 69 mm I.D. × 554 m long pipeline

From the above two figures 3.14 and 3.15 it is found that same material conveying through same pipeline if the pressure tapping location changes the numerical value of Stokes number to allocate PMC also changes. For figure 3.14 constant Stokes number line ranges between 0.5 to 0.6 and figure 3.15 constant Stokes number line ranges between 0.7 to 0.9 allocates the PMC.

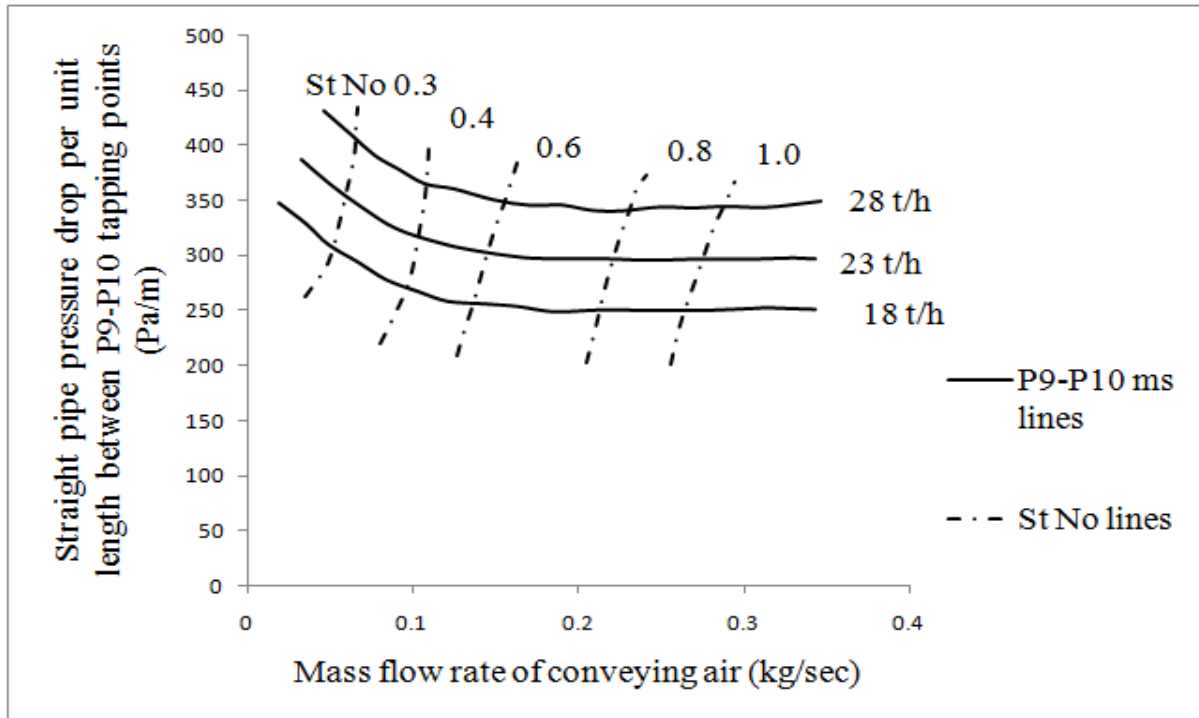


Figure 3.16: PCC for straight pipe (40.10 m) pressure (P_9 - P_{10}), fly ash, 105 mm I.D. \times 168 m long pipeline

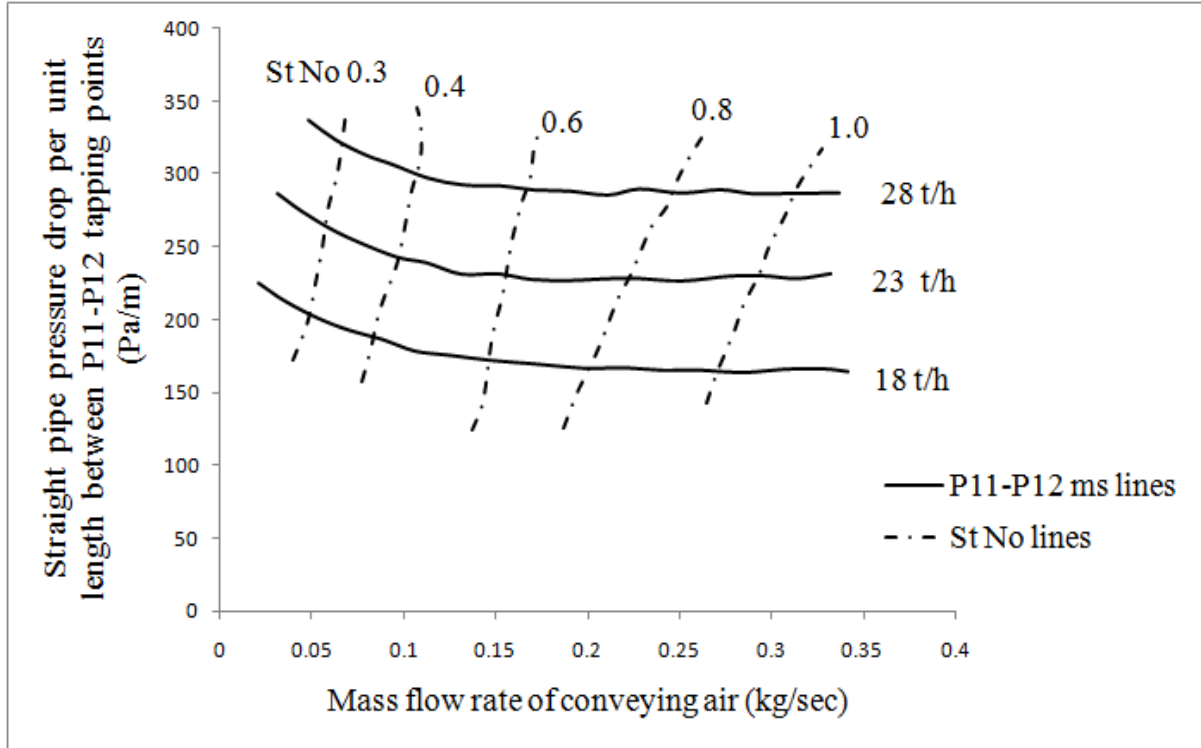


Figure 3.17: PCC for straight pipe (44.50 m) pressure (P_{11} - P_{12}), fly ash, 105 mm I.D. \times 168 m long pipeline

From the above two figure 3.16 and 3.17 it is found that same material is conveyed through same pipeline if the pressure tapping location changes the range of Stokes number surprisingly but does not change to allocate PMC. For figure 3.16 and 3.17 constant Stokes number line ranges between 0.4 to 0.5 indicate the PMC. This is may be due to the scale up of diameter. So, it can be concluded that for diameter scale up condition a unique range of Stokes number could be responsible for allocating PMC irrespective of pressure tapping points throughout the pipeline.

3.5 Constant Stokes number lines plotted on total pipeline PCC

Application of "total pipeline" static pressure measurement data from the respective pipelines and tapping locations over a large bandwidth of steady-state conveying condition, the PCC for the total pipeline sections were obtained for various bulk solids flow rate

- a) Cement, 65 mm I.D. × 254 m long pipeline
- b) Cement, 80 mm I.D. × 407 m long pipeline
- c) Fly ash, 65 mm I.D. × 254 m long pipeline
- d) Fly ash, 80 mm I.D. × 407 m long pipeline
- e) Fly ash, 69 mm I.D. × 168 m long pipeline
- f) Fly ash, 69 mm I.D. × 554 m long pipeline

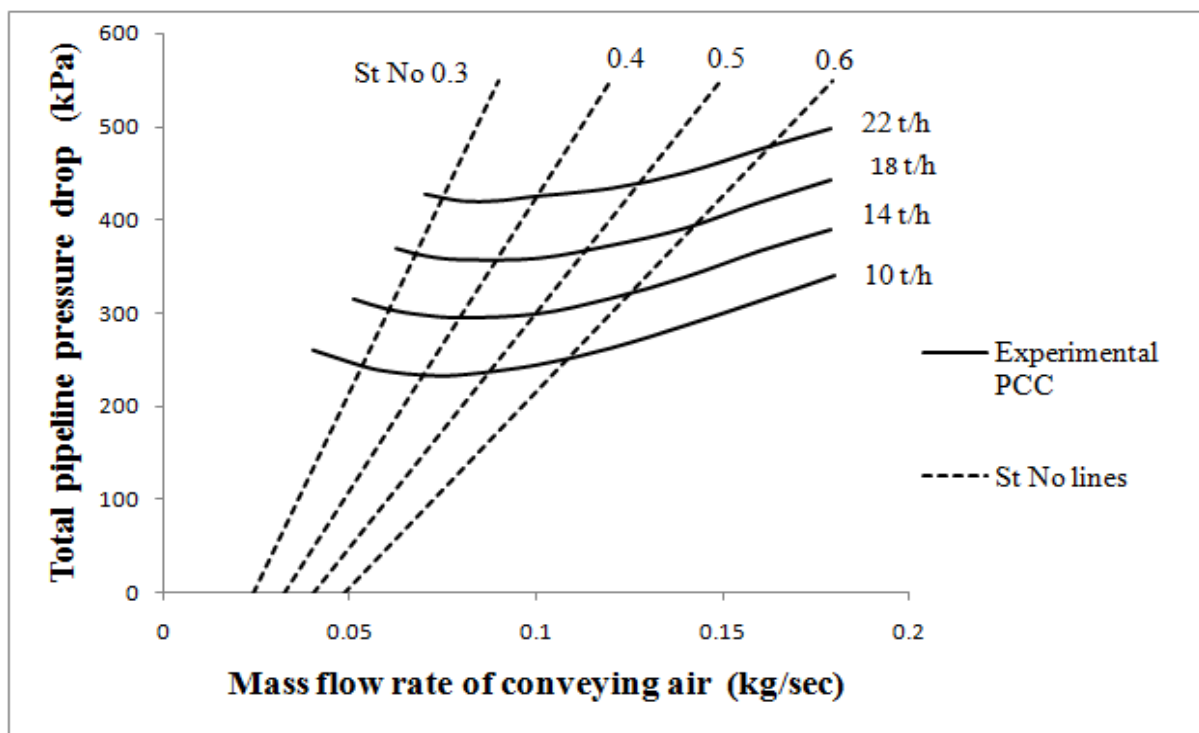


Figure 3.18: PCC for cement, 65 mm I.D. × 254 m long pipeline

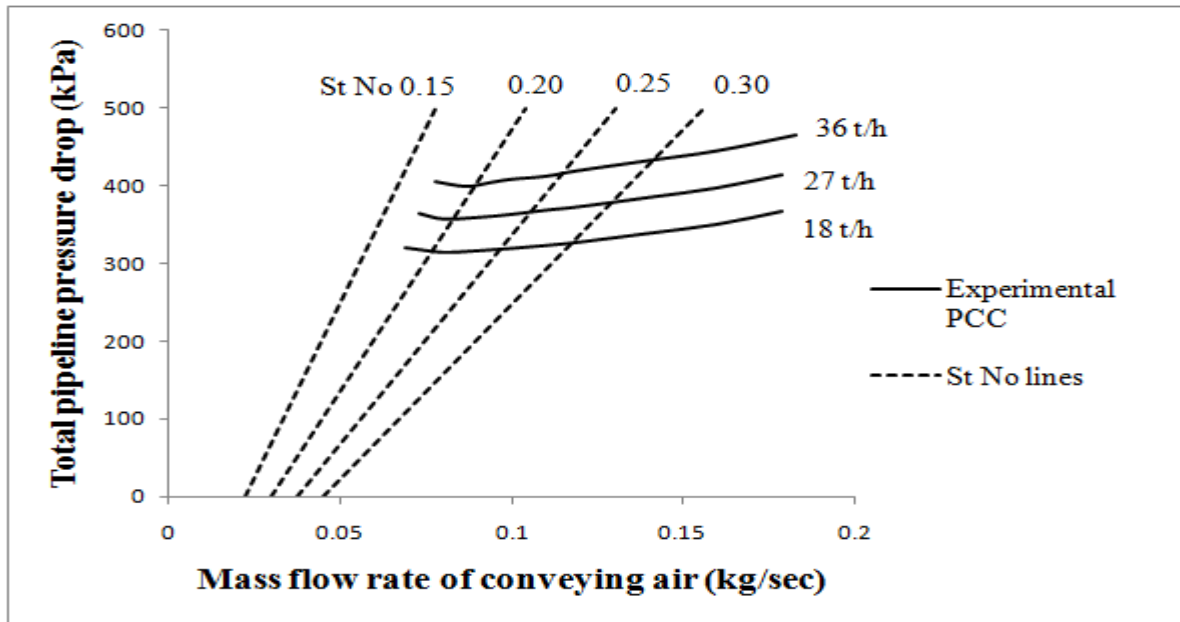


Figure 3.19: PCC for cement, 80 mm I.D. x 407 m long pipeline

From the above two figure 3.18 and 3.19 it shows that same material conveying through different pipeline diameter and length constant Stokes number line ranges between 0.4 to 0.5 and 0.25 to 0.30 allocates the PMC for total pipeline PCC.

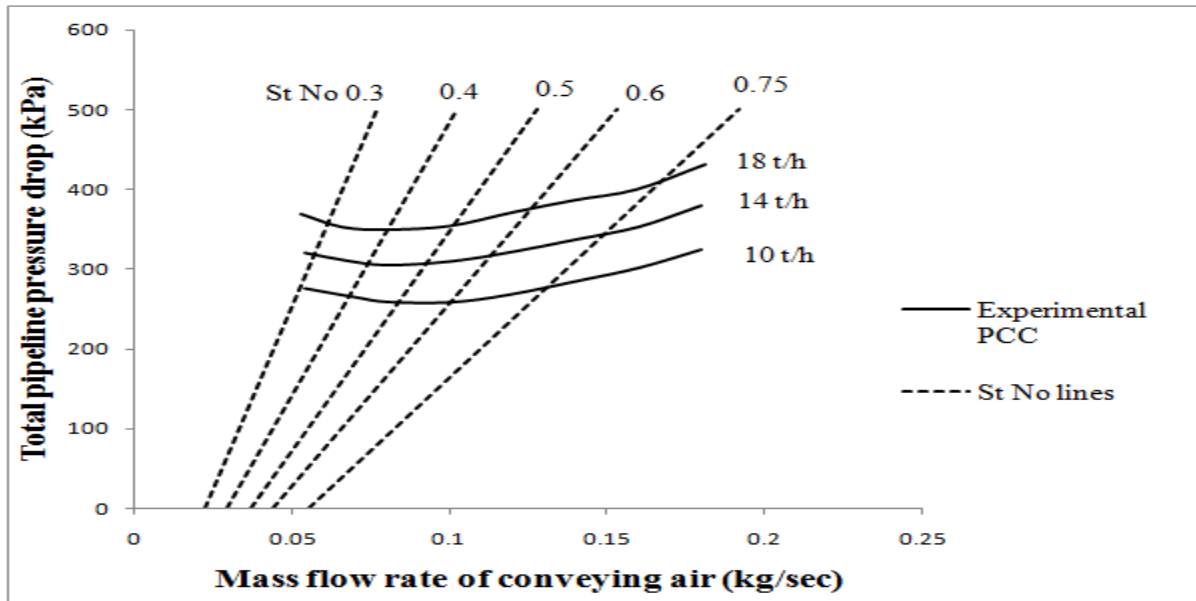


Figure 3.20: PCC for fly ash, 65 mm I.D. x 254 m long pipeline

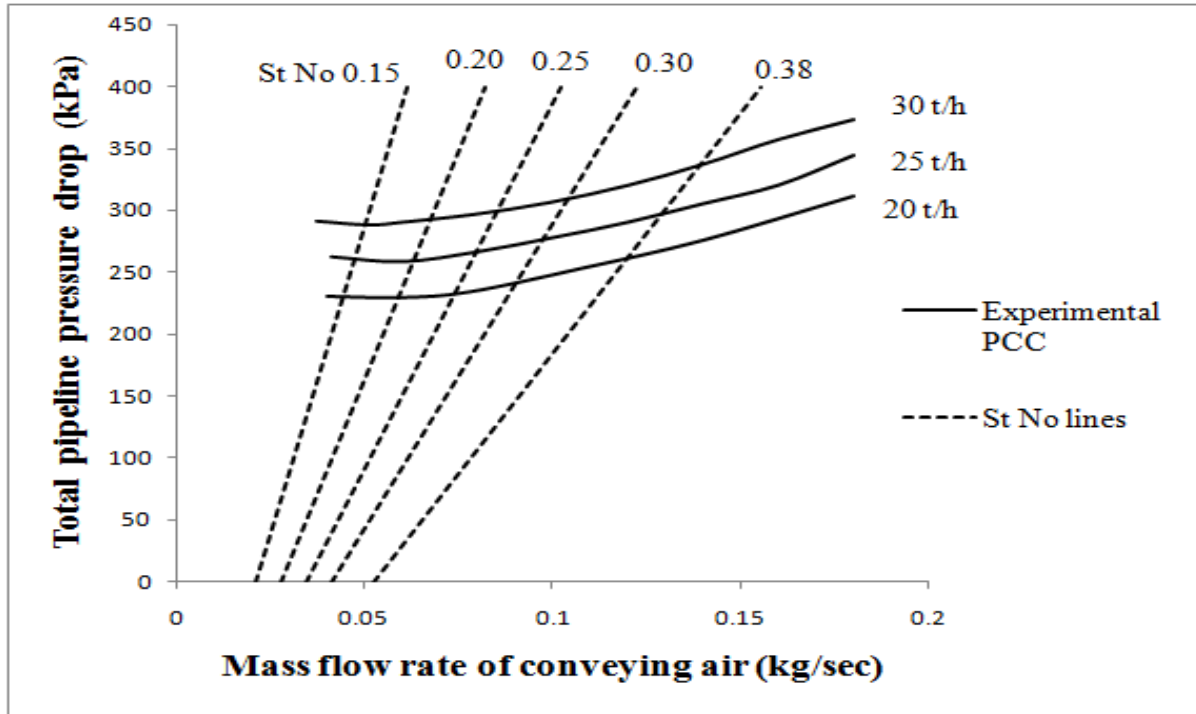


Figure 3.21: PCC for fly ash, 80 mm I.D. × 407 m long pipeline

From the above two figure 3.20 and 3.21, it shows that same material conveyed through different pipelines of different diameter and length, for figure 3.20 and 3.21 constant Stokes number line ranges between 0.4 to 0.5 and 0.20 to 0.25 allocates the PMC respectively for total pipeline PCC.

So, from above four figures it can be concluded that for 65 m I.D. × 254 m long pipeline of unique range of Stokes number 0.4 to 0.5 allocates the PMC irrespective of the conveying material. Similarly, for 80 mm I.D. × 407 m long pipeline of unique range of Stokes number value 0.20 to 0.30 allocates the PMC irrespective of the conveying material.

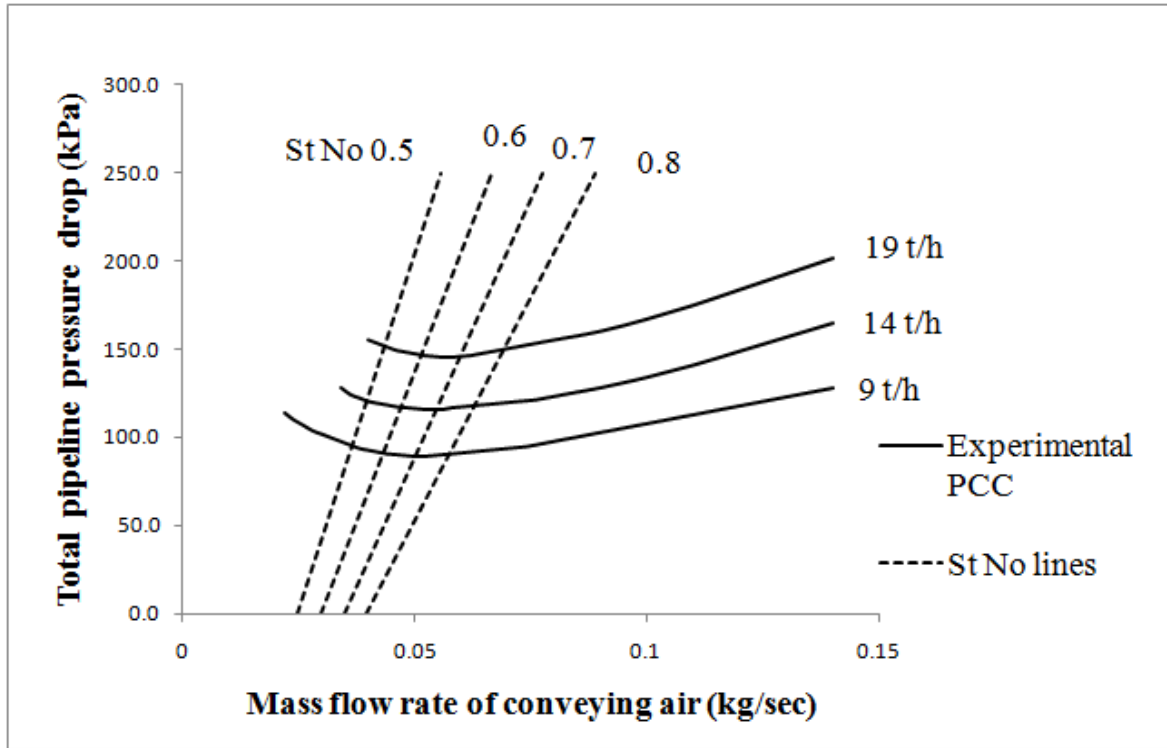


Figure 3.22: PCC for fly ash, 69 mm I.D. × 168 m long pipeline

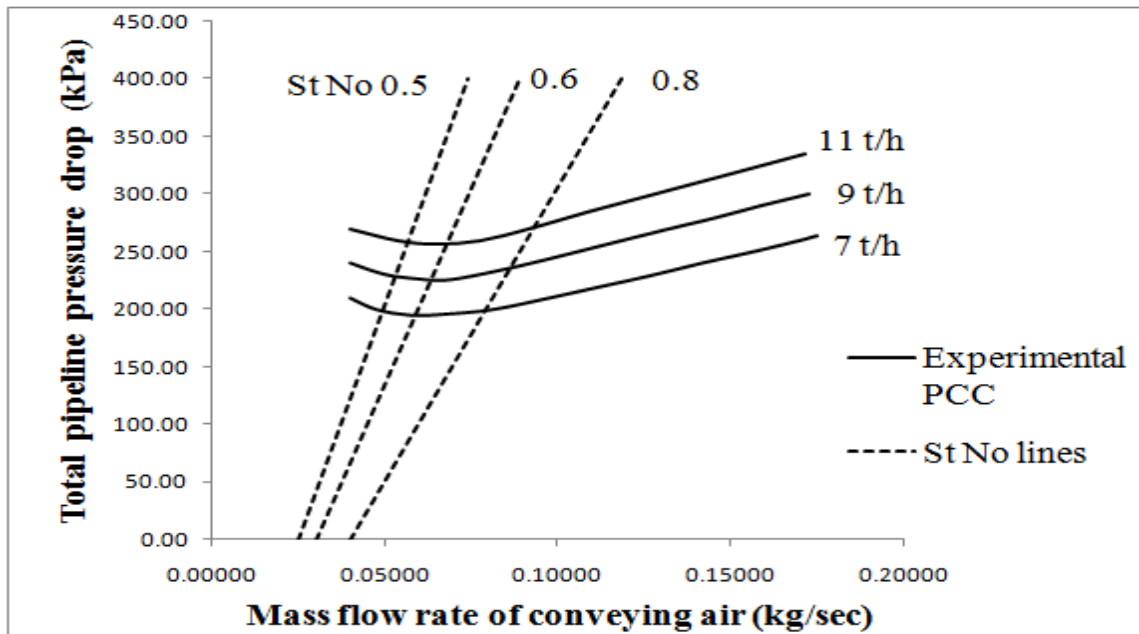


Figure 3.23: PCC for fly ash, 69 mm I.D. × 554 m long pipeline

From the above two figure 3.23 and 3.24 it shows that same material conveying through same pipeline diameter but different length, for figure 3.23 and 3.24 constant Stokes number line 0.6 indicates the PMC. So, it can be concluded that for total pipeline PCC to define dense to dilute phase transition with Stokes number, does not depend upon pipeline length for the pipe of same diameter. That's why for both the cases we got a unique value of Stokes number 0.6.

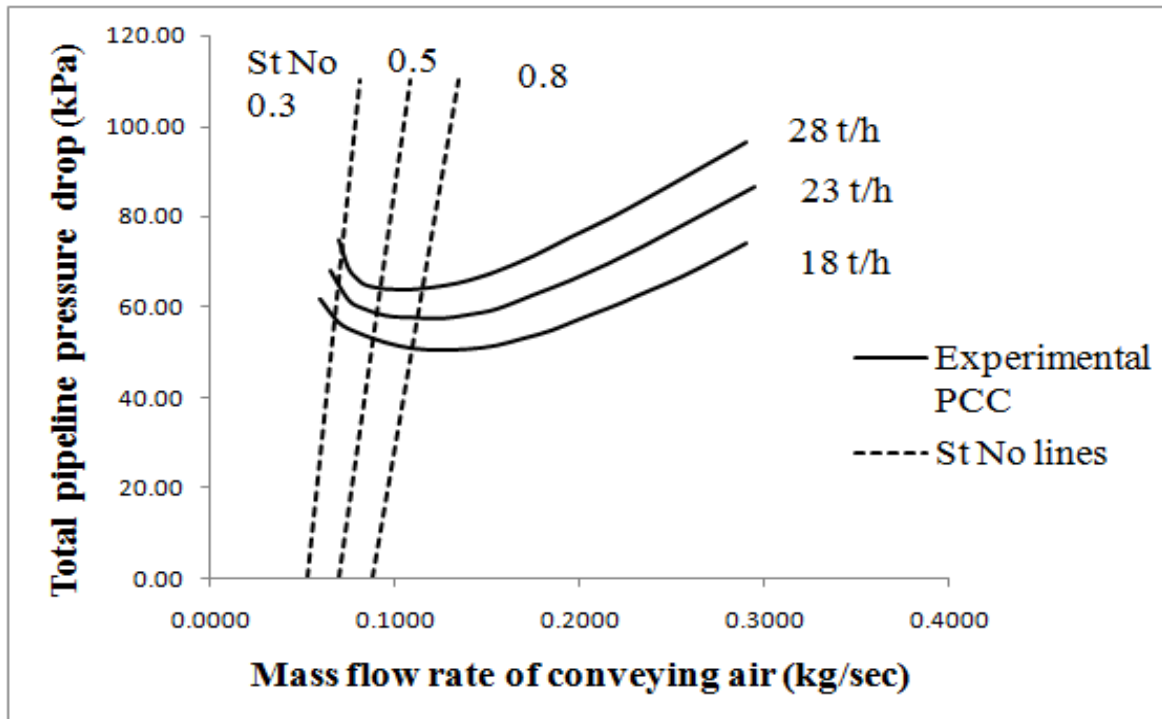


Figure 3.24: PCC for fly ash, 105 mm I.D. × 168 m long pipeline

From the above figure 3.25 constant Stokes number line 0.5 indicates the PMC. So, from above three figures it can be concluded that the numerical value of Stokes number decreases under step-up condition to define dense to dilute phase transition.

Chapter 4

Modeling and Validation of Solids Friction Factor

4.1 Development of new model

Substantial conceptual and experimental work has been done to predict the pressure drop in a gas-solids mixture through a pipeline, but an authentic general correlation has not yet been generated. So, the aim is to propose a reliable modeling and scale-up method for the precise prediction of pressure drop for dense as well as dilute phase pneumatic conveying of fine powders. During gas and solids particles flow through the horizontal pipe when the gas velocity is high enough to keep the particles homogeneously suspended throughout the pipeline then only ideal dilute phase flow exists but for bulk solids transport it is not economic. Due to decrease in gas velocity below the saltation velocity a non-uniform dispersion of solids over the cross-section of the conveying pipe. So, a moving strand is often observed at the bottom of the pipeline. The range of flow pattern observed during pneumatic conveying of bulk materials depends on the material characteristics (particle size, size distribution, shape, hardness and density). Fine powders, such as PVC powder, fly ash, cement, fine coal and carbon fine etc. can be transported in fluidized or moving bed flow at low gas velocities. Immature dune flow is basically the beginning stage of complete dune flow. Froude number is defined as the ratio of inertia force to gravity force and it is not sufficient to model particle-particle/wall interaction for a non-suspension layer. Stokes number is basically represents a particle's flow in a particular fluid. Relaxation time of particle (τ), fluid velocity (V) and a characteristic dimension of the obstacle obstructing the fluid flow (d) is the parameter to determine Stokes number. Particle response time or the relaxation time is a measure of the responsiveness of the particle to a change in gas velocity. Particle diameter (d_p), particle density (ρ_p) and dynamic viscosity of surrounding fluid (μ) are the parameters to determine the relaxation time. The distance a particle would penetrate into a stagnant gas before stopping is $U_o\tau_p$. Where U_o is the initial particle velocity.

The distance is called the stopping distance. The terminal velocity of a particle falling through a stagnant gas $g\tau_p$. Where τ_p can be calculated by ρ_d , d_d^2 and μ_c . Mathematically τ_p is equal to $\rho_d d_d^2 / 18 \mu_c$. Recently the quantification of turbulence statistics due to fine particles has been discussed with the help of Stokes number. Turbulence channel flow is characterized by the flow Reynolds number as well as the length and time scale of turbulence. This is because the turbulent flows are miscellaneous multi scale phenomena. If the particles are introduced in to the turbulence channel flows, the following important quantities must also be considered:

- Ratio of particle density to fluid density
- The particle Reynolds number
- The drag co-efficient of particles
- The ratio of the particle diameter to the length scale of turbulence
- The ratio of particle time scale to the time scale of turbulence i.e. the Stokes number

The turbulence flows with particles are complicated, multi-scale, multi-physics phenomena.

Stokes number = Characteristics time of particle/Characteristics time of flow

$$St\ no = \rho_d d_d^2 V_s / 18 \mu_c D$$

For $St\ no \ll 1$, particle follow the continuous phase flow closely

For $St\ no > 1$, particles unaffected by continuous phase flow

4.2 Immature dune flow

Fine powders, such as PVC powder, fly ash, cement, fine coal and carbon fine etc. can be conveyed in fluidized dense phase. Immature dune flow is basically the beginning stage of complete dune flow. In immature dune flow condition the average conveying medium velocity is such that the conveying particles just tend to terminate. For, modeling solid friction factor to immature dune flow condition solid loading ratio, terminal velocity of particle and average conveying medium velocity are the most important parameter.

For immature dune flow there are some assumptions:

1. There is no isolated clear boundary between suspension and non-suspension layer
2. Maximum amount of conveying air with solids moves through the suspension layer

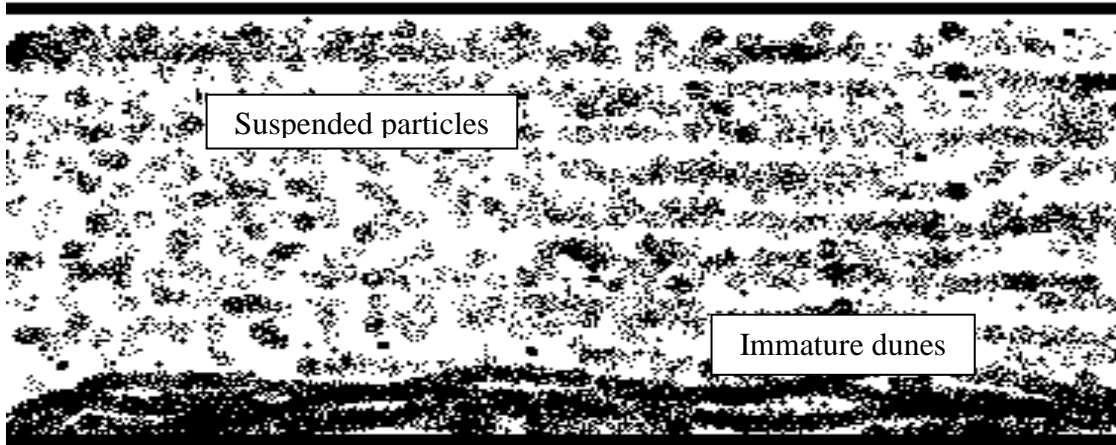


Figure 4.1: Immature dune flow of fine Powders in partially dense-phase conveying

The "Immature dune flow" modeling format can be represented as

$$\lambda_s = K (m^*)^a (g\tau_p/V)^b$$

This model (Eq. 4.1 to Eq. 4.6) is validated over three sets of pipeline including length and diameter step-up condition for conveying cement and fly ash.

$$\text{Model i: } \lambda_s = 45765.08 (m^*)^{-0.9109} (g\tau_p/V)^{2.12} \quad [R^2 = 0.9869] \quad (4.1)$$

for fly ash 65 mm I.D. × 300 m long pipeline. (Fujian Longking Co.)

$$\text{Model ii: } \lambda_s = 3584.44 (m^*)^{-0.6317} (g\tau_p/V)^{1.814} \quad [R^2 = 0.9794] \quad (4.2)$$

for cement 65 mm I.D. × 300 m long pipeline. (Fujian Longking Co.)

$$\text{Model iii: } \lambda_s = 257.59 (m^*)^{-0.5567} (g\tau_p/V)^{1.4143} \quad [R^2 = 0.9721] \quad (4.3)$$

for cement 80 mm I.D. × 407 m long pipeline. (Fujian Longking Co.)

$$\text{Model iv: } \lambda_s = 82.55 (\text{m}^*)^{-0.441} (\text{g}\tau_p/V)^{1.281} \quad [R^2 = 0.9849] \quad (4.4)$$

for fly ash 80 mm I.D. × 407 m long pipeline. (Fujian Longking Co.)

$$\text{Model v: } \lambda_s = 6018.06 (\text{m}^*)^{-0.745} (\text{g}\tau_p/V)^{2.126} \quad [R^2 = 0.9938] \quad (4.5)$$

for fly ash 69 mm I.D. × 168 m long pipeline. (University of Wollongong)

$$\text{Model vi: } \lambda_s = 792.73 (\text{m}^*)^{-0.6406} (\text{g}\tau_p/V)^{1.870} \quad [R^2 = 0.9629] \quad (4.6)$$

for fly ash 69 mm I.D. × 554 m long pipeline. (University of Wollongong)

The above high value of R^2 represent that the compatibility between experimental and predicted values of solids friction factor is superior for all the models.

4.3 Total pipeline predicted PCC according to "Immature dune flow model"

Application of "total pipeline" static pressure measurement data from the respective pipelines and tapping locations over a large bandwidth of steady-state conveying condition, the experimental PCC for the total pipeline and by "Immature dune flow model" the predicted PCC for total pipe line sections were obtained for various bulk solids flow rate

- a) Cement, 65 mm I.D. × 254 m long pipeline
- b) Fly ash, 65 mm I.D. × 254 m long pipeline
- c) Cement, 80 mm I.D. × 407 m long pipeline
- d) Fly ash, 80 mm I.D. × 407 m long pipeline
- e) Fly ash, 69 mm I.D. × 168 m long pipeline
- f) Fly ash, 69 mm I.D. × 554 m long pipeline

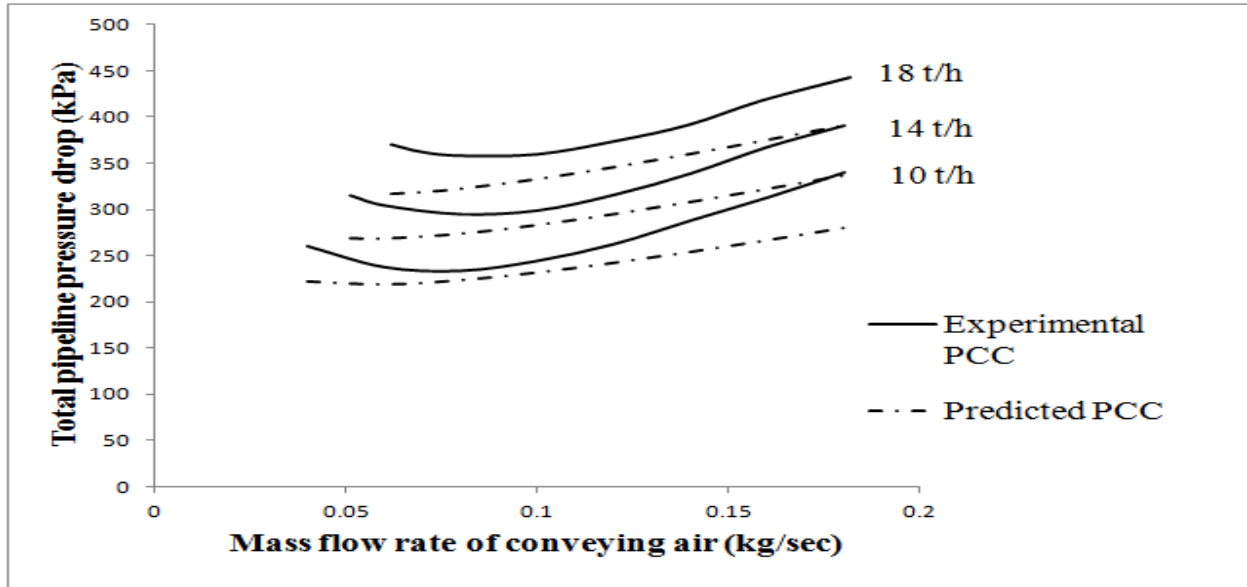


Figure 4.2: Experimental versus predicted PCC for cement 65 mm I.D. × 254 m long pipeline

In the above figure, there exist three m_s lines from top 18 t/h to bottom 10 t/h. According to "Immature dune flow model" there are little under prediction of pressure drop with respect to the experimental pressure drop for conveying of cement.

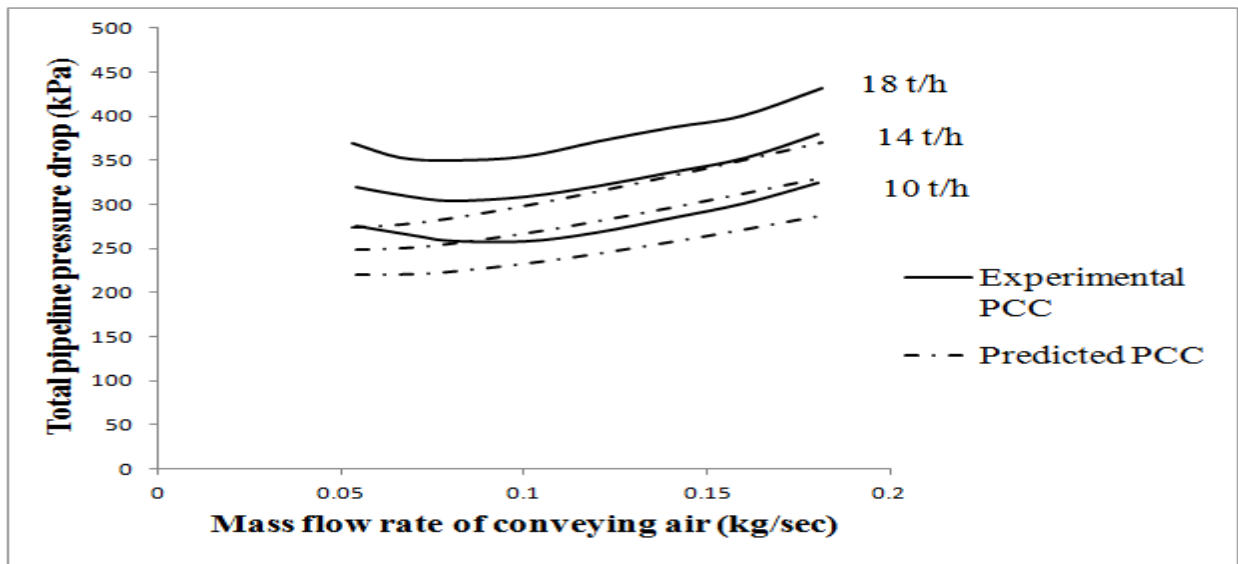


Figure 4.3: Experimental versus predicted PCC for fly ash 65 mm I.D. × 254 m long pipeline

In the above figure, there exist three m_s lines from top 18 t/h to bottom 10 t/h. According to "Immature dune flow model" there are drastic under prediction of pressure drop with respect to the experimental pressure drop for conveying of fly ash. Comparing above two figures 4.2 and 4.3 it can be concluded that for conveying cement and fly ash through the same pipeline predicted PCC is nearer to the experimental PCC in case of cement. The reason may be due to change in mean particle diameter. Mean particle diameter of fly ash ($d_p = 22 \mu\text{m}$) is $3 \mu\text{m}$ more than cement ($d_p = 19 \mu\text{m}$). Where, terminal velocity of particle depends on mean particle diameter.

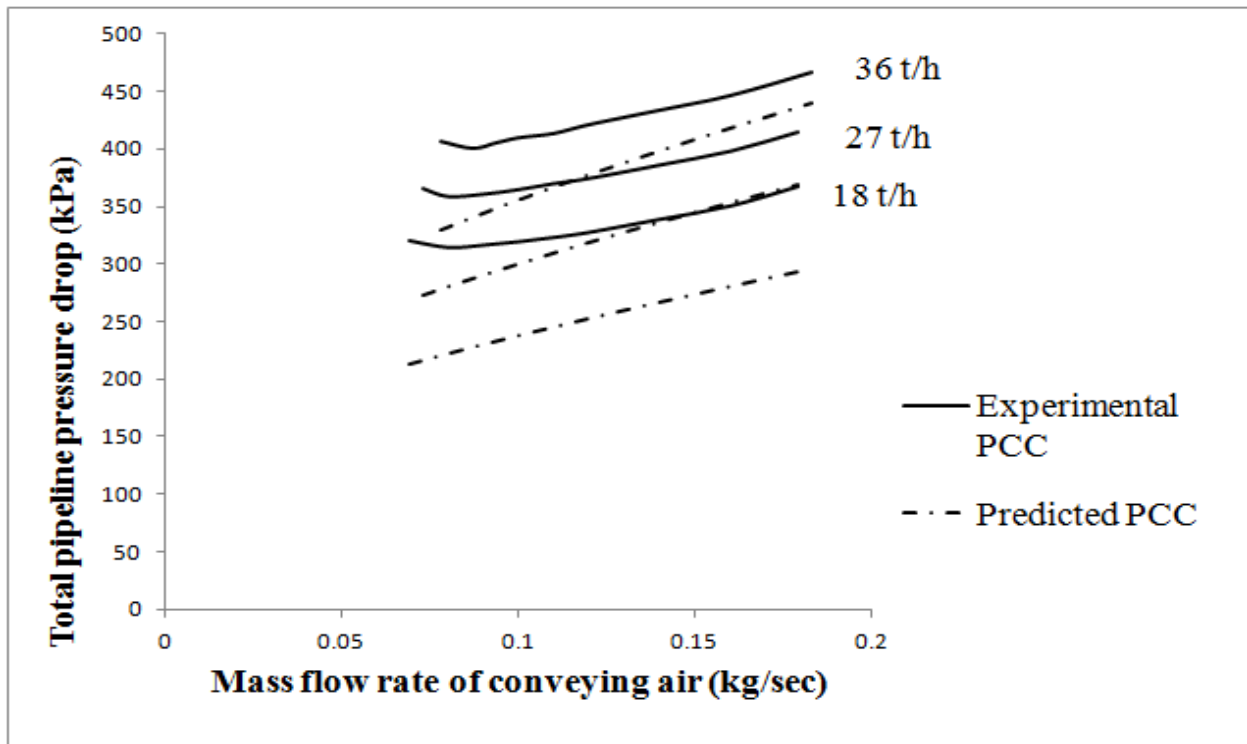


Figure 4.4: Experimental versus predicted PCC for cement 80 mm I.D. \times 407 m long pipeline

In the above figure, there exist three m_s lines from top 36 t/h to bottom 18 t/h. According to "Immature dune flow model" there are drastic under prediction of pressure drop with respect to the experimental pressure drop for conveying of cement.

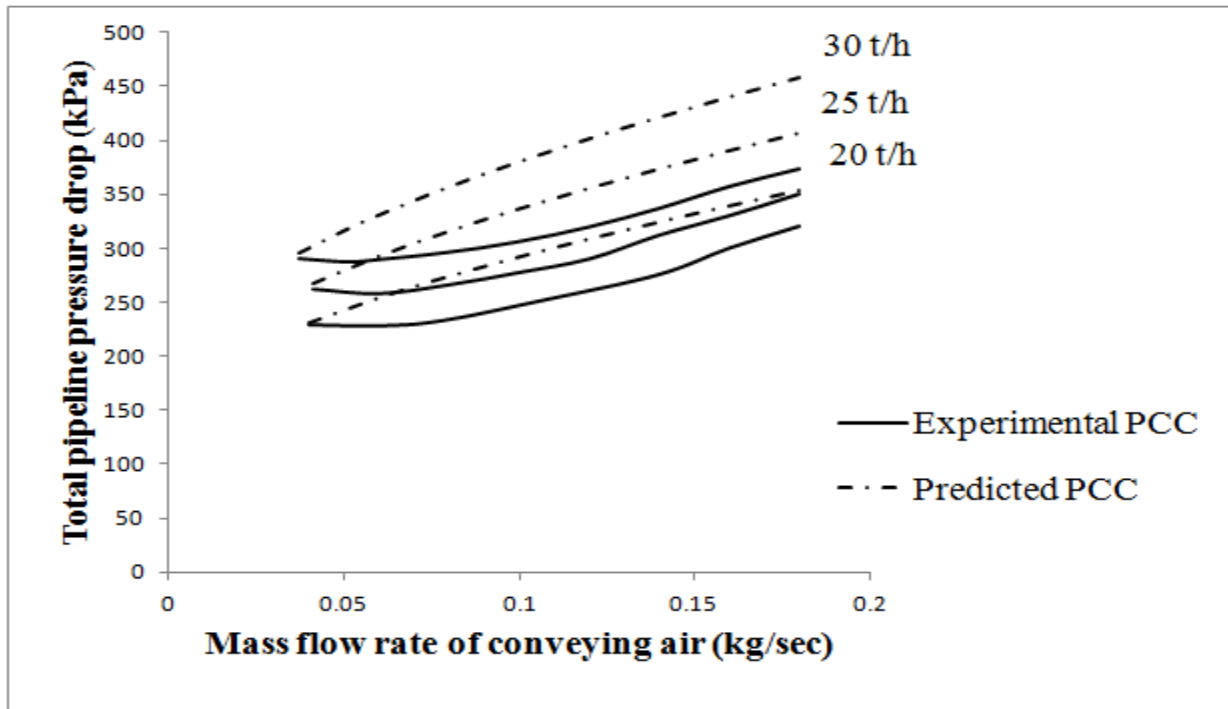


Figure 4.5: Experimental versus predicted PCC for fly ash 80 mm I.D. × 407 m long pipeline

In the above figure, there exist three m_s lines from top 30 t/h to bottom 20 t/h. According to "Immature dune flow model" there are drastic over prediction of pressure drop with respect to the experimental pressure drop for conveying of cement. Surprisingly, it is observed that when the mass flow rate of conveying air is nearer to 0.04 kg/sec, predicted PCC shows nearly accurate prediction of pressure drop to the experimental pressure drop.

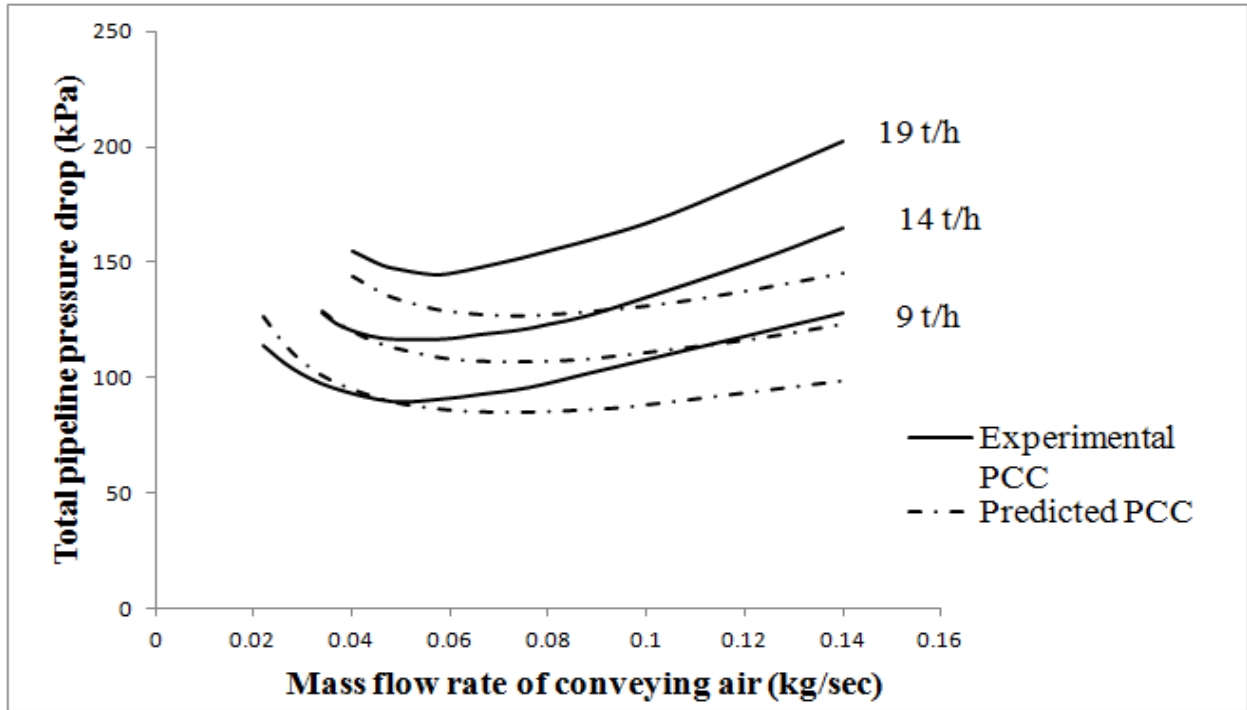


Figure 4.6: Experimental versus predicted PCC for fly ash dust 69 mm I.D. × 168 m long pipeline

In the above figure, there exist three m_s lines from top 19 t/h to bottom 9 t/h. According to "Immature dune flow model" there are drastic under prediction of pressure drop with respect to the experimental pressure drop for conveying of fly ash in dilute phase region. However, in dense phase region when the mass flow rate of conveying air changes from 0.02 to 0.05 kg/sec predicted PCC shows nearly accurate prediction of pressure drop with respect to the experimental pressure drop.

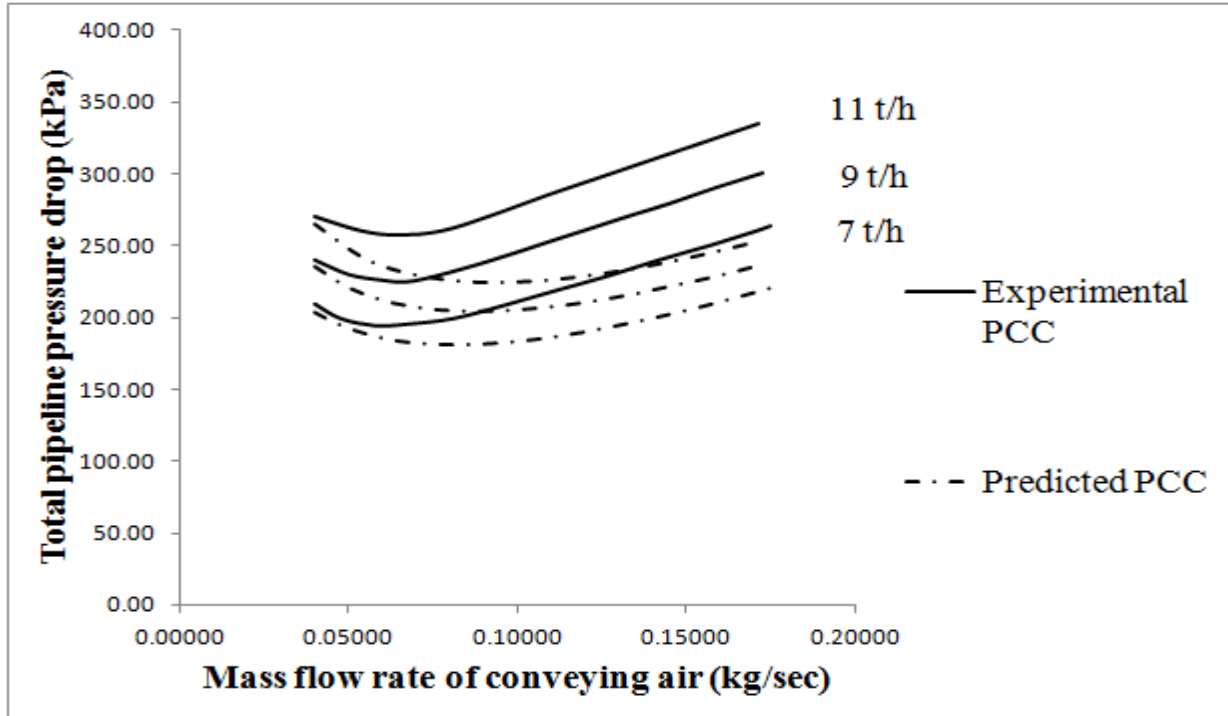


Figure 4.7: Experimental versus predicted PCC for fly ash dust 69 mm I.D. × 554 m long pipeline

In the above figure, there exist three m_s lines from top 11 t/h to bottom 7 t/h. According to "Immature dune flow model" there are drastic under prediction of pressure drop with respect to the experimental pressure drop for conveying of fly ash in dilute phase region. Where as in dense phase region when the mass flow rate of conveying air changes from 0.035 to 0.048 kg/sec predicted PCC shows nearly accurate prediction of pressure drop with respect to the experimental pressure drop.

4.4 Two layer flow

According to two-layer model suspended solid particles are moved over the non-suspended partially static layer. In case of moving bed flow a dune type pattern on the bed surface could be observed. It has been noticed that the depth of the suspension and non-suspension are not always constant throughout the pipe length, but the depth varies throughout the length. Basically, at the very beginning of the pipeline where the velocity is very less the gas solids move in the form of plug. As the mass-flow rate of solids increases in suspension layer particle/particle/wall interaction increases and that causes high energy losses. However, according to definition of Stokes number it is very much sufficient to model particle-particle/wall interaction for a non-suspension layer. “Weber-A4” model provides good prediction of pressure drop for dilute phase flow for several pipeline arrangement. According to this model the total solids friction loss has two independent loss component- losses due to impact and friction between particle-particle/air/pipe wall interactions and that due to retaining the particles in suspension.

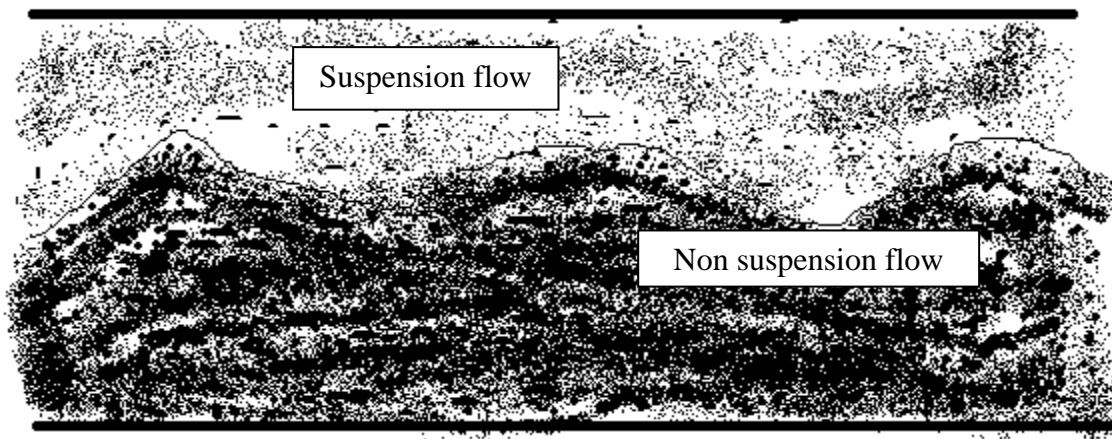


Figure 4.8: Two-Layer Flow of Fine Powders in Dense-Phase

The model, as showed by Wypych et al. (1990) is represented by (Eq. 4.7)

$$\lambda_s = \lambda_s^* C/V + 2\beta_0/[(C/V) Fr^2] \quad (4.7)$$

where, $\beta_0 = w_{fo}/V$ and w_{fo} is the free settling velocity of an isolated particle. This basically refers the condition when the motion of a single particle is not influenced by the motion of the

surrounding particles. That's why this model is very much suitable for dilute phase flow. One auxiliary problem with this approach is to address a data point towards the dilute-phase range for the value of λ_s^* to properly represent the suspension layer. Therefore, a "two-layer" based model can be applied to combine the above two modeling techniques. However, according to "Modified two-layer modeling format" for calculating the solids friction factor, where the weight factor τ_1 and τ_2 can be represented by Stokes number based criteria (from St no {min} = 0.025 to St no {max} = 1.75).

The "Modified Two-Layer Modeling Format" can be represented as (Eq. 4.8)

$$\lambda_s = \tau_1 [K (m^*)^a (St \text{ no})^b (\rho_s/\rho_f)^c] + \tau_2 (\lambda_s^* C/V + 2\beta_0/[(C/V) Fr^2]) \quad (4.8)$$

Where; K, a, b are constants and τ_1 and τ_2 are weighing factors which can be defined as (Eq. 4.9 and 4.10)

$$\tau_1 = \{ 1 - [(St \text{ no mean} - St \text{ no minimum}) / (St \text{ no maximum} - St \text{ no minimum})] \} \quad (4.9)$$

$$\tau_2 = [(St \text{ no mean} - St \text{ no minimum}) / (St \text{ no maximum} - St \text{ no minimum})] \quad (4.10)$$

New "Two- Layer modeling format" was again validated for 6 sets of PCC (2 products, 4 pipelines) (Eq. 4.11 to Eq. 4.16)

For Two-Layer model there are some assumptions:

1. Suspension and non-suspension layer is isolated by a clear boundary
2. Maximum amount of conveying air with solids moves through the non-suspension layer
3. Non-suspension layer behaves like a single phase flow having uniform value of apparent density and viscosity throughout the thickness of non-suspension layer

$$\text{Model i: } \lambda_s = 0.01309 (m^*)^{-0.793} (\text{St no})^{-1.95} (\rho_p/\rho_f)^{0.208} \quad [R^2 = 0.9895] \quad (4.11)$$

for fly ash 65 mm I.D. × 300 m long pipeline. (Fujian Longking Co.)

$$\text{Model ii: } \lambda_s = 0.01105 (m^*)^{-0.568} (\text{St no})^{-1.721} (\rho_p/\rho_f)^{0.1112} \quad [R^2 = 0.9807] \quad (4.12)$$

for cement 65 mm I.D. × 300 m long pipeline. (Fujian Longking Co.)

$$\text{Model iii: } \lambda_s = 0.00280 (m^*)^{-0.491} (\text{St no})^{-1.367} (\rho_p/\rho_f)^{0.262} \quad [R^2 = 0.9827] \quad (4.13)$$

for cement 80 mm I.D. × 407 m long pipeline. (Fujian Longking Co.)

$$\text{Model iv: } \lambda_s = 0.0182 (m^*)^{-0.4401} (\text{St no})^{-1.279} (\rho_p/\rho_f)^{0.0078} \quad [R^2 = 0.9849] \quad (4.14)$$

for fly ash 80 mm I.D. × 407 m long pipeline. (Fujian Longking Co.)

$$\text{Model iii: } \lambda_s = 0.05316 (m^*)^{-0.7217} (\text{St no})^{-2.095} (\rho_p/\rho_f)^{0.0818} \quad [R^2 = 0.9938] \quad (4.15)$$

for fly ash 69 mm I.D. × 168 m long pipeline. (University of Wollongong)

$$\text{Model iv: } \lambda_s = 0.01929 (m^*)^{-0.5703} (\text{St no})^{-1.7756} (\rho_p/\rho_f)^{0.1220} \quad [R^2 = 0.9634] \quad (4.16)$$

for fly ash 69 mm I.D. × 554 m long pipeline. (University of Wollongong)

The above high value of R^2 represent that the compatibility between experimental and predicted values of solids friction factor is superior for all the models.

4.5 Total pipeline predicted PCC according to “Modified two-layer theory”

Application of "total pipeline" static pressure measurement data from the respective pipelines and tapping locations over a large bandwidth of steady-state conveying condition, the experimental PCC for the total pipeline and by “Modified two-layer theory” the predicted PCC for total pipe line sections were obtained for various bulk solids flow rate

- a) Cement, 65 mm I.D. × 254 m long pipeline
- b) Fly ash, 65 mm I.D. × 254 m long pipeline
- c) Cement, 80 mm I.D. × 407 m long pipeline
- d) Fly ash, 80 mm I.D. × 407 m long pipeline
- e) Fly ash, 69 mm I.D. × 168 m long pipeline
- f) Fly ash, 69 mm I.D. × 554 m long pipeline

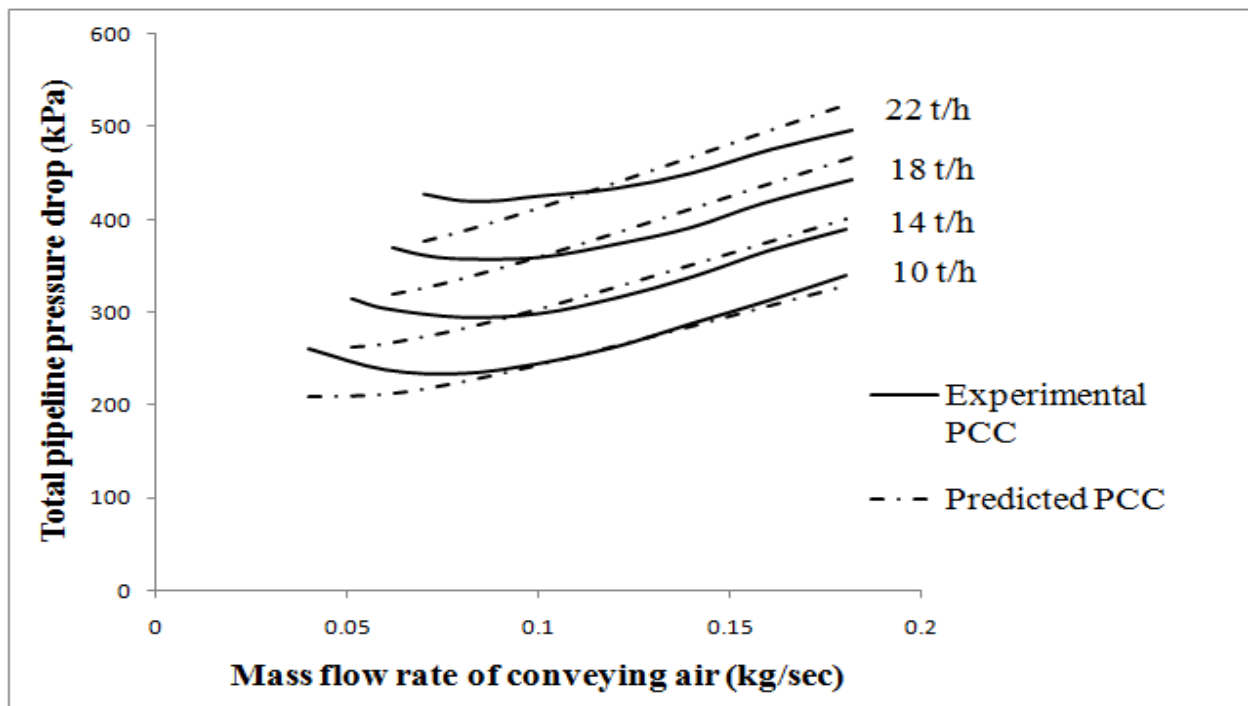


Figure 4.9 Experimental versus predicted PCC for cement 65 mm I.D. × 254 m long pipeline

In the above figure, there exist four m_s lines from top 22 t/h to bottom 10 t/h. According to new model there are little over predictions for all the tonnage lines. The trend of predicted PCC according to “Modified two-layer theory” shows a mild increase in predicted pressure drop as the mass flow rate of conveying air increases for dilute phase region. In dense phase region the predicted PCC shows slightly more under prediction. Mass flow rate of conveying air from 0.08 to 0.18 kg/sec the predicted PCC shows nearly accurate prediction of experimental PCC for calculating pressure drop.

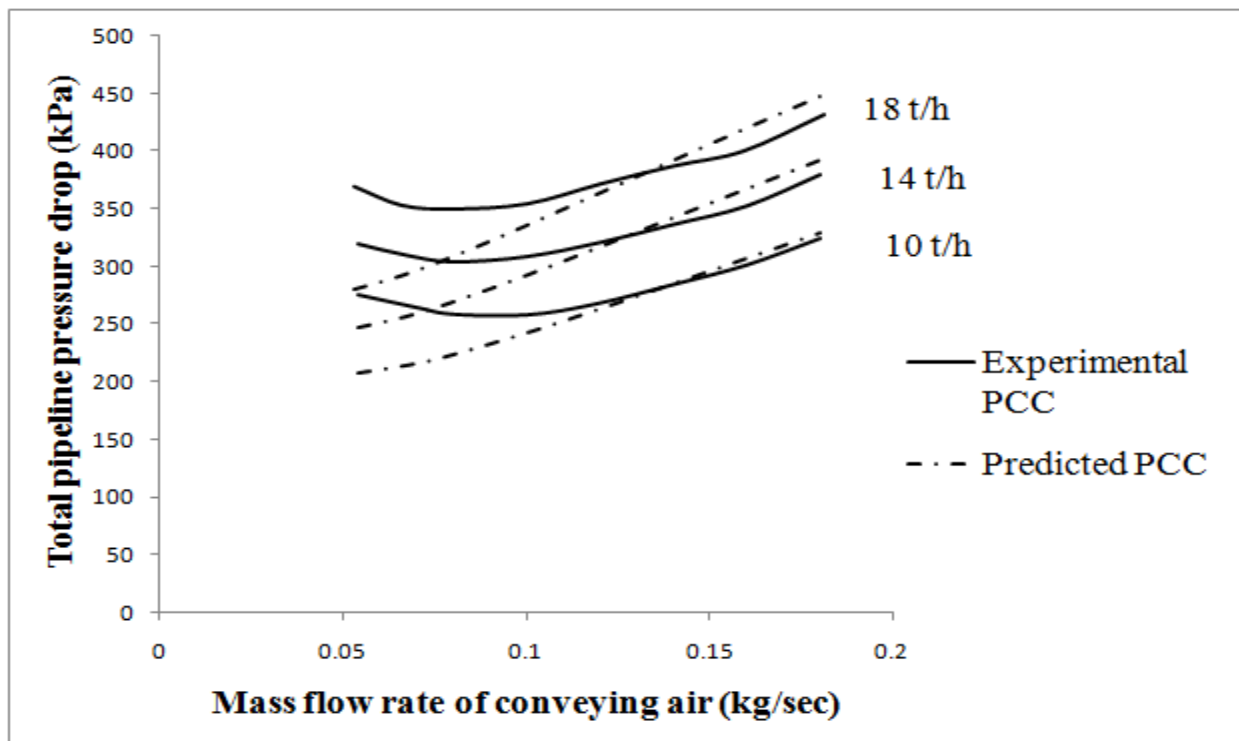


Figure 4.10: Experimental versus predicted PCC for fly ash 65 mm I.D. × 254 m long pipeline

In the above figure, continuous line represents experimental PCC and dotted line represents predicted PCC. From top 18 t/h to bottom 10 t/h. The trend of predicted PCC according to “Modified two-layer theory” shows a mild increase in predicted pressure drop as the mass flow rate of conveying air increases for dilute phase region. In dense phase region the predicted PCC shows under prediction. Mass flow rate of conveying air from 0.11 to 0.18 kg/sec the predicted

PCC shows nearly accurate prediction of experimental PCC for calculating pressure drop. So, by analyzing above two figures 4.9 and 4.10 it can be concluded that for the same pipeline irrespective of conveying material conveyed the predicted PCC shows nearly accurate prediction of pressure drop in dilute phase region. Predicted PCC shows little under prediction in dense phase region.

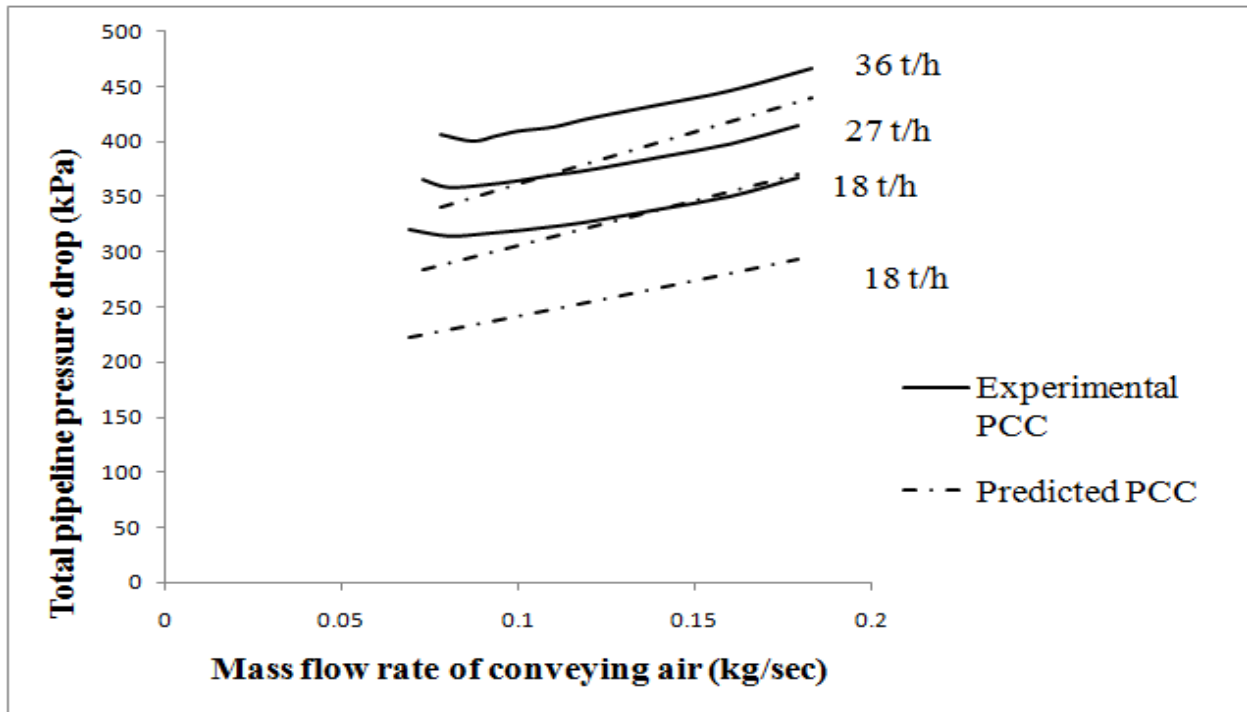


Figure 4.11: Experimental versus predicted PCC for cement 80 mm I.D. × 407 m long pipeline

In the above figure, continuous line represents experimental PCC and dotted line represents predicted PCC. The top line represents $m_s = 36$ t/h, middle line represents $m_s = 27$ t/h and bottom line represents $m_s = 18$ t/h. For conveying cement through a step-up pipe line, there is a more under prediction of pressure drop for predicted PCC. That indicates the new model is not very much reliable for step-up diameter condition.

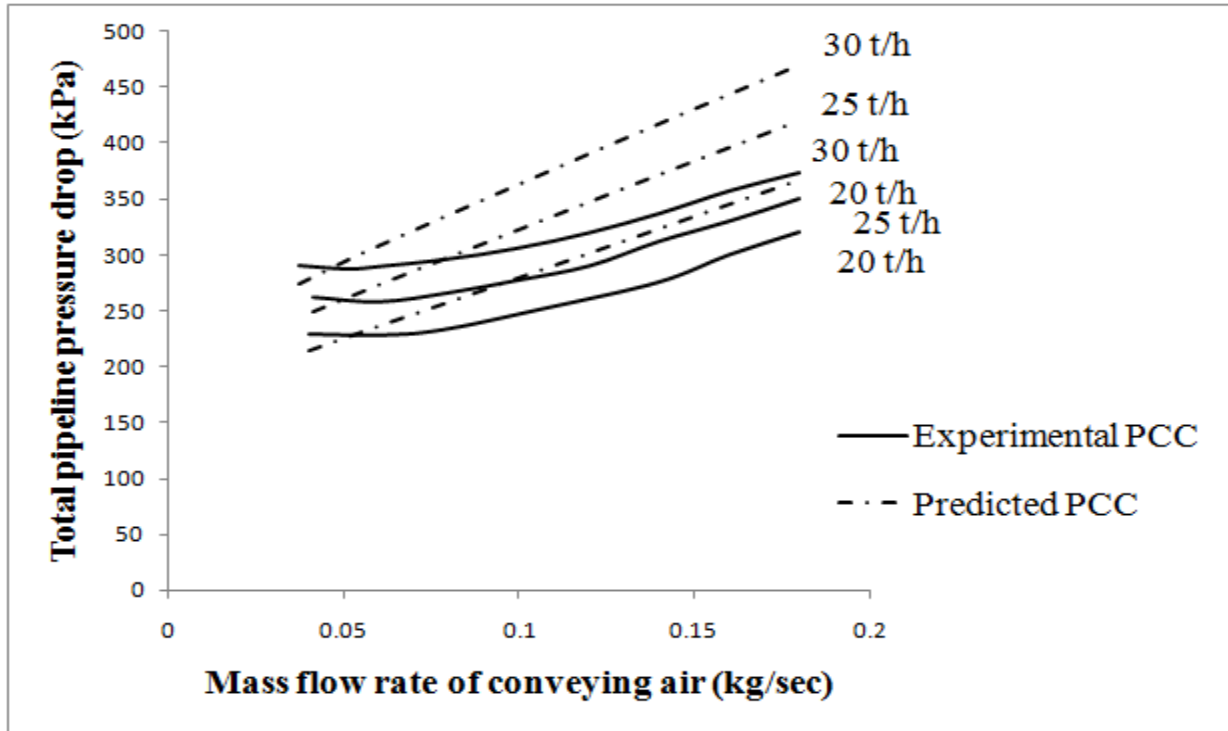


Figure 4.12: Experimental versus predicted PCC for fly ash 80 mm I.D. \times 407 m long pipeline

In the above figure, continuous line represents experimental PCC and dotted line represents predicted PCC. The top line represents $m_s = 30$ t/h, middle line represents $m_s = 25$ t/h and bottom line represents $m_s = 20$ t/h. According to new model for conveying fly ash through a step-up pipe line, there is an over prediction of pressure-drop in dilute phase region. However, surprisingly the predicted PCC shows nearly accurate prediction of pressure drop in dense phase region, when the mass flow rate of conveying air changes from 0.04 to 0.053 kg/sec. That indicates the new model is not suitable for step-up in diameter condition also.

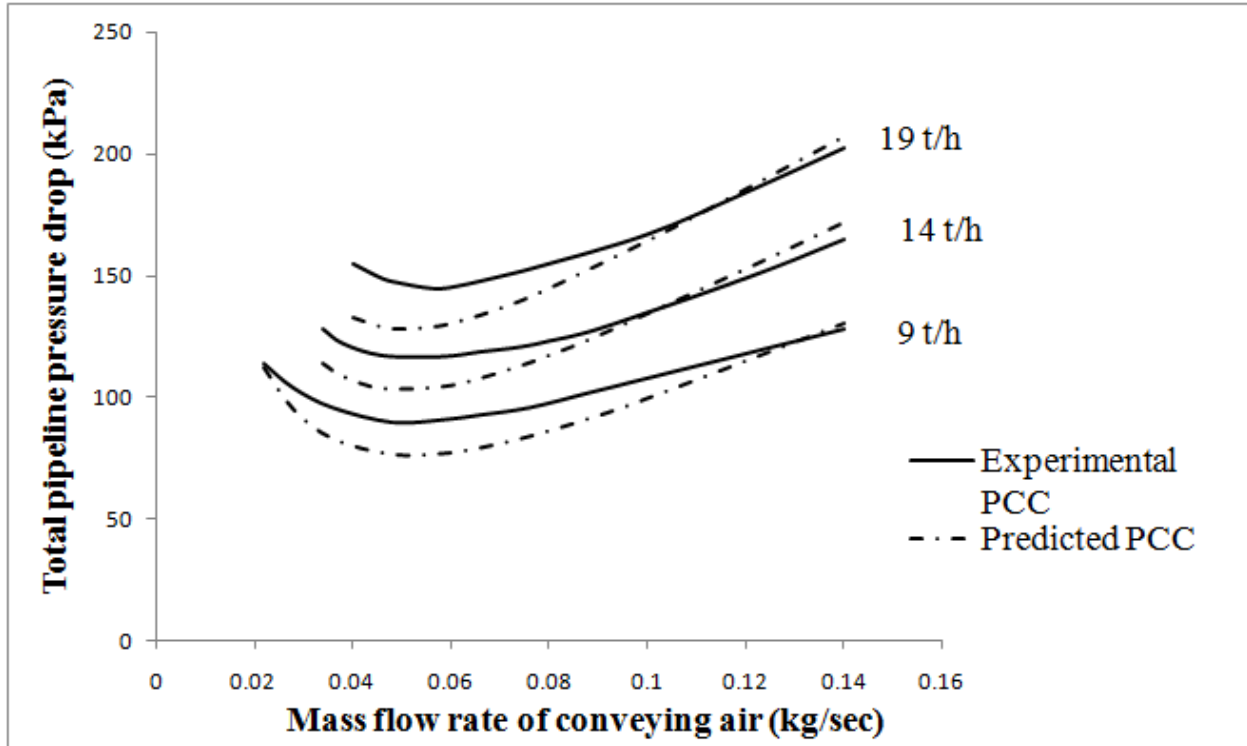


Figure 4.13: Experimental versus predicted PCC for fly ash dust 69 mm I.D. × 168 m long pipeline

In the above figure, continuous line represents experimental PCC and dotted line represents predicted PCC. The top line represents $m_s = 19$ t/h, middle line represents $m_s = 14$ t/h and bottom line represents $m_s = 9$ t/h. According to new model there are nearly accurate predictions of pressure drop when the mass flow rate of conveying air changes from 0.1 to 0.142 kg/sec. Whereas mass flow rate of conveying air ranges between 0.022 to 0.1 kg/sec the predicted PCC shows little under prediction.

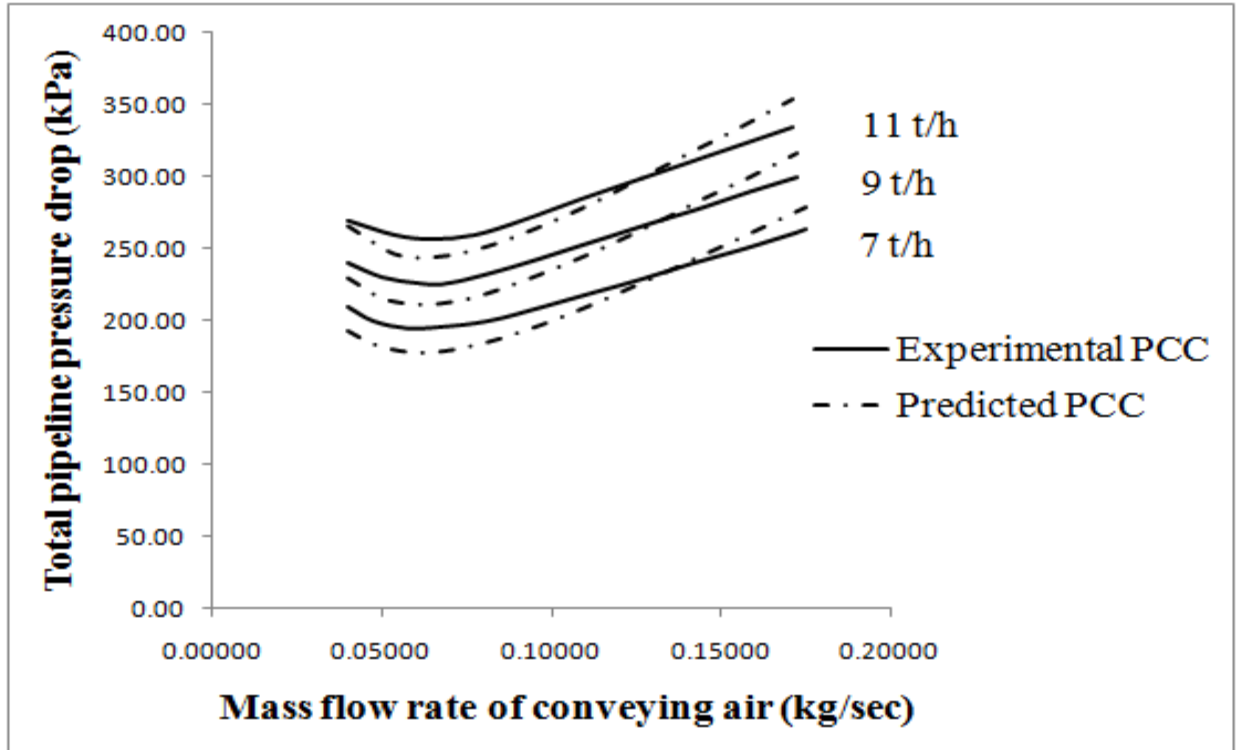


Figure 4.14: Experimental versus predicted PCC for fly ash dust 69 mm I.D. × 554 m long pipeline

In the above figure, continuous line represents experimental PCC and dotted line represents predicted PCC. The top line represents $m_s = 11$ t/h, middle line represents $m_s = 9$ t/h and bottom line represents $m_s = 7$ t/h. Comparing above two figures 4.13 and 4.14 conveying fly ash through the same pipeline diameter but step-up in length condition "Modified two-layer theory" provides nearly accurate prediction of pressure drop in dense as well as dilute phase.

Chapter 5

Conclusion and Future Scope of Work

5.1 Conclusion

Straight pipe PCC are generally flattish type, it is very difficult to define the PMC on the straight pipe PCC. To address the transition in flow mechanism from dense to dilute phase along the flow direction it is very important to indicate the PMC on the straight pipe PCC. Based on the experimental data analysis for conveying two different fine powders along four different pipeline (including step-up of diameter and length), it can be predicted that constant Stokes number line ranges from 0.4 to 0.5 indicating the PMC and in this range of Stokes number, constant m^* line varies from 40 to 50. To predict the pressure drop, two distinct approach have been introduced to model solids friction factor. One approach is based on solid loading ratio, Stokes number and density of conveying medium to the particle density of solids. Other approach is based on solid loading ratio and terminal velocity of particle to the average velocity of the conveying medium. Where, terminal velocity calculated by multiplication of characteristics time of particle (τ_p) to the gravitational acceleration (g), "Modified two-layer theory" provides better prediction of pressure drop on dilute phase region. However, significantly under prediction is found in dense phase region. However, "Immature Dune flow model" provides nearly accurate prediction of pressure drop in dense phase region but with drastic under prediction of pressure drop in dilute phase region with respect to experimental pressure drop.

5.2 Future scope of work

Further scope of work will comprises:

- a) An effort has been made to address dense to dilute phase transition in straight pipe PCC for conveying of fine powders, but, still there is a requirement of development of a unique model to address transition in flow mechanism from dense to dilute phase in a straight pipe PCC for conveying of fine as well as coarse powders.
- b) Further work must be done to develop a unique solids friction factor model for both dense and dilute phase to predict the pressure drop throughout the pipeline.

References

- Bansal, A., Mallick, S.S. and Wypych, P.W., 2013. Investigating straight-pipe pneumatic conveying characteristics for fluidized dense-phase pneumatic conveying. *Particulate Science and Technology*, 31(4), pp.348-356.
- Behera, N., Agarwal, V.K., Jones, M.G. and Williams, K.C., 2013. CFD modeling and analysis of dense phase pneumatic conveying of fine particles including particle size distribution. *Powder technology*, 244, pp.30-37.
- Behera, N., Agarwal, V.K., Jones, M.G. and Williams, K.C., 2013. Modeling and analysis of dilute phase pneumatic conveying of fine particles. *Powder technology*, 249, pp.196-204.
- Benyahia, S., Syamlal, M. and O'Brien, T.J., 2005. Evaluation of boundary conditions used to model dilute, turbulent gas/solids flows in a pipe. *Powder Technology*, 156(2), pp.62-72.
- Cabrejos, F.J. and Klinzing, G.E., 1994. Pickup and saltation mechanisms of solid particles in horizontal pneumatic transport. *Powder technology*, 79(2), pp.173-186.
- Chambers, A.J. and Marcus, R.D., 1986. Pneumatic conveying calculations. In *Second International Conference on Bulk Materials Storage, Handling and Transportation: 1986; Preprints of Papers* (p. 49). Institution of Engineers, Australia.
- El-Behery, S.M., Hamed, M.H., El-Kadi, M.A. and Ibrahim, K.A., 2009. CFD prediction of air–solid flow in 180 curved duct. *Powder Technology*, 191(1), pp.130-142.
- Elghobashi, S., 1994. On predicting particle-laden turbulent flows. *Applied Scientific Research*, 52(4), pp.309-329.
- Geldart, D. and Ling, S.J., 1992. Saltation velocities in high pressure conveying of fine coal. *Powder Technology*, 69(2), pp.157-162.

- Heinl, E. and Bohnet, M., 2005. Calculation of particle–wall adhesion in horizontal gas–solids flow using CFD. *Powder Technology*, 159(2), pp.95-104.
- Hilton, J.E. and Cleary, P.W., 2011. The influence of particle shape on flow modes in pneumatic conveying. *Chemical engineering science*, 66(3), pp.231-240.
- Jones, M.G. and Williams, K.C., 2003. Solids friction factors for fluidized dense-phase conveying. *Particulate Science and Technology*, 21(1), pp.45-56.
- Kalman, H., Satran, A., Meir, D. and Rabinovich, E., 2005. Pickup (critical) velocity of particles. *Powder Technology*, 160(2), pp.103-113.
- Klinzing, G.E., Myler, C.A., Zaltash, A. and Dhodapkar, S., 1989. A simplified correlation for solids friction factor in horizontal conveying systems based on Yang's unified theory. *Powder technology*, 58(3), pp.187-193.
- Klinzing, G.E., Rizk, F., Marcus, R. and Leung, L.S., 2011. *Pneumatic conveying of solids: a theoretical and practical approach (Vol. 8)*. Springer Science & Business Media.
- Mallick, S.S. and Wypych, P.W., 2009. Minimum transport boundaries for pneumatic conveying of powders. *Powder Technology*, 194(3), pp.181-186.
- Mallick, S.S. and Wypych, P.W., 2010. An investigation into modeling of solids friction for dense-phase pneumatic conveying of powders. *Particulate Science and Technology*, 28(1), pp.51-66.
- Mason, D.J. and Levy, A., 2001. A model for non-suspension gas–solids flow of fine powders in pipes. *International Journal of Multiphase Flow*, 27(3), pp.415-435.
- McGlinchey, D., Cowell, A., Knight, E.A., Pugh, J.R., Mason, A. and Foster, B., 2007. Bend pressure drop predictions using the Euler-Euler model in dense phase pneumatic conveying. *Particulate Science and Technology*, 25(6), pp.495-506.
- Pan, R. and Wypych, P.W., 1992. Scale-up procedures for pneumatic conveying design. *Powder Handling and Processing*, 4, pp.167-167.

- Rabinovich, E. and Kalman, H., 2007. Pickup, critical and wind threshold velocities of particles. *Powder Technology*, 176(1), pp.9-17.
- Rizk, F., 1982. Pneumatic transport in dilute and dense phase. *Bulk Solids Handling*, 2(2), pp.9-15.
- Setia, G. and Mallick, S.S., 2015. Modelling fluidized dense-phase pneumatic conveying of fly ash. *Powder Technology*, 270, pp.39-45.
- Setia, G., Mallick, S.S. and Wypych, P.W., 2014. On improving solid friction factor modeling for fluidized dense-phase pneumatic conveying systems. *Powder Technology*, 257, pp.88-103.
- Setia, G., Mallick, S.S., Pan, R. and Wypych, P.W., 2015. Modeling minimum transport boundary for fluidized dense-phase pneumatic conveying systems. *Powder Technology*, 277, pp.244-251.
- Stegmaier, W., 1978. Zur berechnung der horinentalen pneumatischen forderung feinkorniger feststoffe-for the calculation of horizontal pneumatic conveying of fine grained solids. *Fordern and Heben*, 28, pp.363-366.
- Tomita, Y., Agarwal, V.K., Asou, H. and Funatsu, K., 2008. Low-velocity pneumatic conveying in horizontal pipe for coarse particles and fine powders. *Particuology*, 6(5), pp.316-321.
- Triesch, O. and Bohnet, M., 2001. Measurement and CFD prediction of velocity and concentration profiles in a decelerated gas–solids flow. *Powder Technology*, 115(2), pp.101-113.
- Wang, F.J., Zhu, J.X. and Beeckmans, J.M., 2000. Pressure gradient and particle adhesion in the pneumatic transport of cohesive fine powders. *International journal of multiphase flow*, 26(2), pp.245-265.
- Weber, M., 1981. Principles of hydraulic and pneumatic conveying in pipes. *Bulk Solids Handling*, 1(1), pp.57-63.

Wypych, P.W. and Arnold, P.C., 1989. Recent engineering developments in the application of pneumatic pipeline transport of bulk solids to Australian industry. In Institution of Engineers, Australia National Conference: 1989; Preprints of Papers, The (p. 332). Institution of Engineers, Australia.

Wypych, P.W. and Hauser, G., 1990. Design considerations for low-velocity conveying systems & pipelines. In Pneumatech 4, Int. Conf. on Pneumatic Conveying Technology (pp. 241-260).

Yi, J., Wypych, P.W. and Pan, R., 1998. Pneumatic Conveying-Minimum Conveying Velocity in Dilute-Phase Pneumatic Conveying. Powder Handling and Processing, 10(3), pp.255-262.

Appendix : A

A. Layout of the test rigs

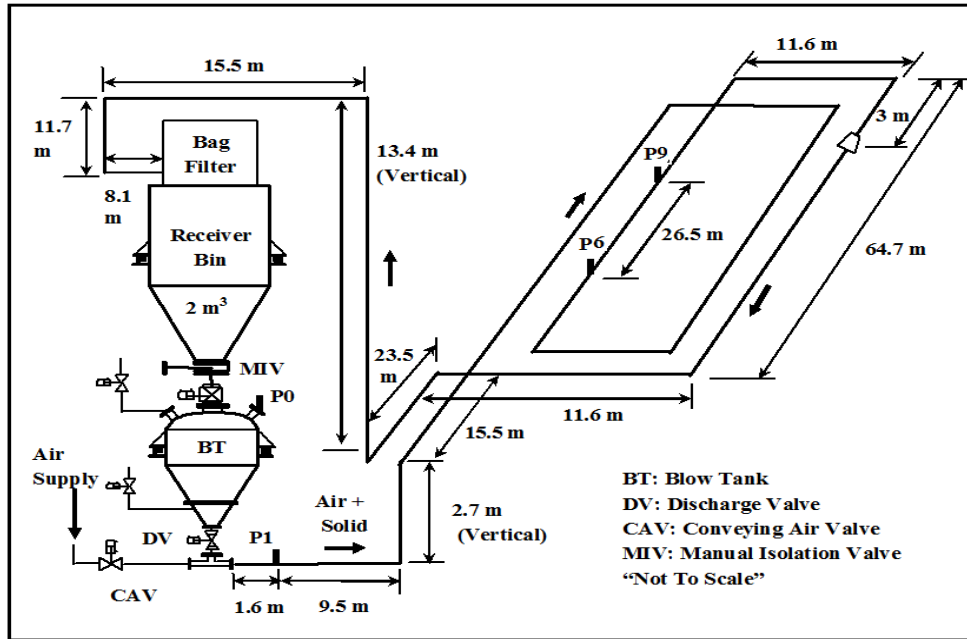


Figure A.1: Layout of the 80 mm I.D. × 407 m long test rig for fly ash and cement

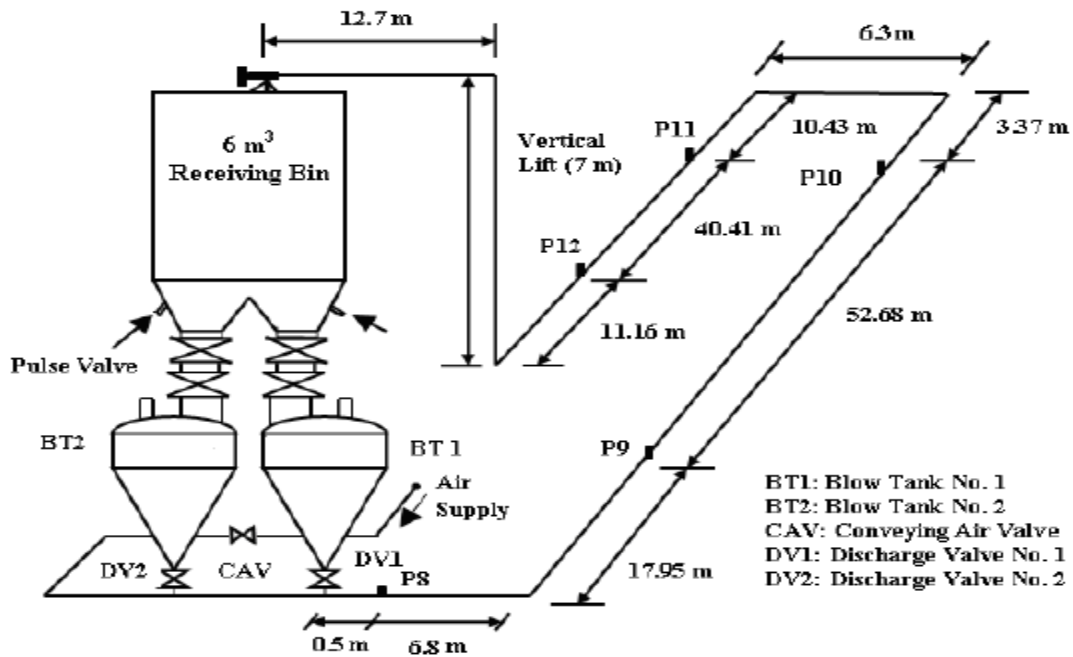


Figure A.2: Layout of the 69 mm I.D. × 168 m long test rig for fly ash

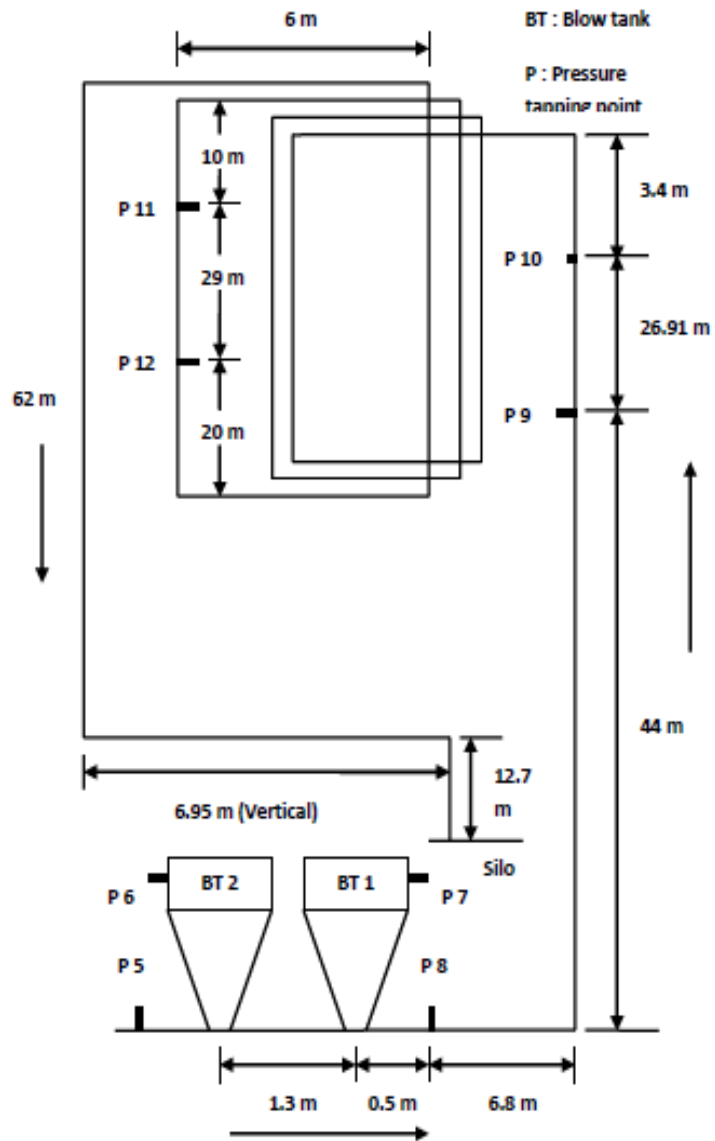


Figure A.3: Layout of the 69 mm I.D. × 55.4 m long test rig for fly ash

Under Progress

Kar, P.K., Setia, G., Mittal, A and Mallick, S.S. An Investigation into the Straight-Pipe Conveying Characteristics and Modeling of Solids Friction Factor for Dense Phase Pneumatic Conveying of Fine Powders.

Prabir

ORIGINALITY REPORT

20%
SIMILARITY INDEX

7%
INTERNET SOURCES

17%
PUBLICATIONS

5%
STUDENT PAPERS

PRIMARY SOURCES

1 S. S. Mallick. "An Investigation into Modeling of Solids Friction for Dense-Phase Pneumatic Conveying of Powders", Particulate Science And Technology, 01/2010 **2%**
Publication

2 Setia, G., S.S. Mallick, R. Pan, and P.W. Wypych. "Modeling solids friction factor for fluidized dense-phase pneumatic transport of powders using two layer flow theory", Powder Technology, 2016. **2%**
Publication

3 Mittal, A., S. S. Mallick, and P. W. Wypych. "An Investigation into the Transition of Flow Mechanism during Fluidized Dense-Phase Pneumatic Conveying of Fine Powders", Particulate Science And Technology, 2015. **1%**
Publication
